Plant Communications
Research article

CellPress
Partner Journal

The proteome landscape of the root cap reveals a role for the jacalin-associated lectin JAL10 in the salt-induced endoplasmic reticulum stress pathway

Krishna Kodappully Das[1], Ankita Mohapatra[1], Abin Panackal George[1], Sreenivas Chavali[1], Katja Witzel[2,*] and Eswarayya Ramireddy[1,*]

[1]Department of Biology, Indian Institute of Science Education and Research (IISER) Tirupati, Tirupati 517507, Andhra Pradesh, India

[2]Leibniz Institute of Vegetable and Ornamental Crops, Theodor-Echtermeyer-Weg 1, 14979 Großbeeren, Germany

***Correspondence: Katja Witzel (witzel@igzev.de), Eswarayya Ramireddy (eswar.ramireddy@iisertirupati.ac.in)**

https://doi.org/10.1016/j.xplc.2023.100726

ABSTRACT

Rapid climate change has led to enhanced soil salinity, one of the major determinants of land degradation, resulting in low agricultural productivity. This has a strong negative impact on food security and environmental sustainability. Plants display various physiological, developmental, and cellular responses to deal with salt stress. Recent studies have highlighted the root cap as the primary stress sensor and revealed its crucial role in halotropism. The root cap covers the primary root meristem and is the first cell type to sense and respond to soil salinity, relaying the signal to neighboring cell types. However, it remains unclear how root-cap cells perceive salt stress and contribute to the salt-stress response. Here, we performed a root-cap cell-specific proteomics study to identify changes in the proteome caused by salt stress. The study revealed a very specific salt-stress response pattern in root-cap cells compared with non-root-cap cells and identified several novel proteins unique to the root cap. Root-cap-specific protein–protein interaction (PPI) networks derived by superimposing proteomics data onto known global PPI networks revealed that the endoplasmic reticulum (ER) stress pathway is specifically activated in root-cap cells upon salt stress. Importantly, we identified root-cap-specific jacalin-associated lectins (JALs) expressed in response to salt stress. A JAL10-GFP fusion protein was shown to be localized to the ER. Analysis of *jal10* mutants indicated a role for JAL10 in regulating the ER stress pathway in response to salt. Taken together, our findings highlight the participation of specific root-cap proteins in salt-stress response pathways. Furthermore, root-cap-specific JAL proteins and their role in the salt-mediated ER stress pathway open a new avenue for exploring tolerance mechanisms and devising better strategies to increase plant salinity tolerance and enhance agricultural productivity.

Key words: Arabidopsis, root cap, cell-type specific proteomics, salt stress, ER stress, jacalin-associated lectin

Das K.K., Mohapatra A., George A.P., Chavali S., Witzel K., and Ramireddy E. (2023). The proteome landscape of the root cap reveals a role for the jacalin-associated lectin JAL10 in the salt-induced endoplasmic reticulum stress pathway. Plant Comm. **4**, 100726.

INTRODUCTION

Agricultural production is severely affected by high soil salinity. Nearly 1.5 million ha of farmland per year is out of crop production because of soil salinization, causing a decrease in production potential of 46 million ha annually (Food and Agriculture Organization of the United Nations, 2020). Several anthropogenic and natural processes, such as over-irrigation, climate change, rainfall, aeolian deposits, mineral weathering, and stored salts, contribute to soil salinity (Rengasamy, 2006). Soluble salt accumulation in the soil severely affects plant growth by inducing osmotic stress and ion toxicity (Munns and Tester 2008; van Zelm et al., 2020). High salt levels in the soil and the plant affect several physiological and

Published by the Plant Communications Shanghai Editorial Office in association with Cell Press, an imprint of Elsevier Inc., on behalf of CSPB and CEMPS, CAS.

biochemical processes during plant growth and development. For example, plants facing salt stress experience reduced photosynthesis, protein synthesis, and lipid metabolism, which result in reduced leaf surface expansion, lower biomass, and reduced growth, thus impeding development (reviewed by Rasool et al., 2013; Yang and Guo, 2018; van Zelm et al., 2020; Fu and Yang, 2023; Shelden and Munns, 2023).

Previous studies have revealed salt-signaling pathways that operate in roots and shoots, from initial salt perception to events that lead to cell death. However, gaps remain to be addressed at every stage of the plant response to salt stress. For example, it is not yet clear how Na^+ enters the cell. Although single channels or transmembrane proteins have not yet been identified, entry of Na^+ ions into plants may occur through non-selective cation channels and the high-affinity K^+ transporter (HKT1) (Essah et al., 2003). The entry of Na^+ ions into cells disturbs water potential and affects Na^+/K^+ ionic homeostasis, thus creating ionic stress. The imbalance in cytosolic ion homeostasis and disturbed water potential lead to a rapid increase in cytosolic Ca^{2+}, primarily in the roots (Knight et al., 1997). This increased Ca^{2+} level helps to maintain ionic homeostasis and reduce osmotic stress (Tracy et al., 2008). For example, the well-studied SOS (salt overly sensitive) pathway is crucial for decoding salt-induced Ca^{2+} signals and restoring the ionic balance. The Na^+/H^+ antiporter SOS1/NHX7 is a crucial player in the evolutionarily conserved SOS pathway. It transports sodium out of the cell with the support of the phosphorylated kinases SOS2 and SOS3 (Guo et al., 2001; Lin et al., 2009). In addition, salt stress leads to activation of channel proteins such as AHA2 (H^+-ATPase), AVP1 (vacuolar H^+-pyrophosphatase), and VAB2 (vacuolar H^+-ATPase subunit) for sequestration of Na^+ ions from the cytoplasm (Gaxiola et al., 2002; Batelli et al., 2007; Duan et al., 2007; Fuglsang et al., 2007). In addition to maintenance of ionic homeostasis, elevated levels of reactive oxygen species (ROS) are brought back to steady-state levels by activating enzymatic and non-enzymatic ROS scavengers. For example, the enzymatic antioxidant catalase 2 (CAT2) shows increased ROS scavenging during salt stress (Song et al., 2021).

Despite progress in our understanding of the plant salt-stress response, the critical driving factor(s) that determine plant responses to salt stress remain elusive (Ismail et al., 2014). One reason for this paucity of knowledge is the complexity of signaling during salt stress: ionic toxicity and osmotic stress may occur in a temporal manner during salt stress (Munns and Tester, 2008), and salt-stress responses differ among different root cell types (Dinneny et al., 2008; Geng et al., 2013). Therefore, understanding the spatiotemporal dynamics of salt responses at the cellular level will unravel the complexity of salt sensing and signaling pathways. To address this topic, we aimed to map the functional players in root-cap cells of *Arabidopsis* under salt stress in a temporal manner.

The root cap, located at the tip of the primary root (PR) in dicots, is at the forefront of sensing and relaying different environmental stimuli for plant growth and adaptation. The role of the root cap in several tropic responses, including gravitropism, halotropism, hydrotropism, and, recently, nutritropism, has been established and envisaged (Kumpf and Nowack, 2015; Kanno et al., 2016; Ganesh et al., 2022). Furthermore, root-cap-derived auxin and cytokinin contribute to PR meristem size and lateral root (LR) development (Xuan et al., 2016; Di Mambro et al., 2019). Root-cap cells are also essential for penetration into the soil and communication with rhizosphere microbiota (Miyasaka and Hawes, 2001; Massa and Gilroy, 2003; Swarup et al., 2005; Kumpf and Nowack, 2015; Kanno et al., 2016; Ganesh et al., 2022). However, it remains unclear how root-cap cells achieve this multitasking, and the proteins and gene regulatory networks that aid in this process are unknown. Because the root cap is the first point of contact, high salt in the soil has been shown to affect the root-cap structure in several crop plants (Qiao 2011; Bogoutdinova et al., 2020; Ninmanont et al., 2021). Thus, investigating the specific functional players in the root cap under salt stress will help us to untangle the complex cellular responses of the root cap.

Here, we characterized the root-cap cell-specific proteome under normal and salt-stress conditions using a promoter:reporter line specific to the columella and LR cap cells. We identified several novel proteins unique to root-cap cells upon salt treatment, and we generated root-cap-specific protein–protein interaction (PPI) networks by superimposing proteomics data onto known PPI networks. These PPI networks revealed that the endoplasmic reticulum (ER) stress pathway is specifically activated in root-cap cells upon salt stress. Furthermore, we identified salt-responsive root-cap-specific jacalin-associated lectins (JALs) in the ER. Functional characterization of one of the JALs, JAL10, revealed that it may alleviate salt stress by regulating the salt-induced ER stress pathway.

RESULTS

Root-cap cell-specific proteomics under salt stress

Previous studies have highlighted the regulatory roles of individual *Arabidopsis root* cell types in developmental and stress responses, significantly advancing our understanding of root plasticity (Brady et al., 2007; Dinneny et al., 2008; Geng et al., 2013; Rich-Griffin et al., 2020). Among root cell types, the root cap (central columella and LR cap cells) is unique for its multifaceted role in plant adaptation (Ganesh et al., 2022). However, a reporter line whose reporter gene is expressed specifically in the root cap is required to explore the role of the root cap. To identify root-cap-specific genes, we performed an *in silico* analysis using the condition search tool of the GENEVESTIGATOR database (Hruz et al., 2014). Candidate genes were shortlisted by cross-comparing their expression profiles using the eFB browser (Winter et al., 2007). Our analysis identified *At5g54370*, which encodes a late embryogenesis abundant protein-like protein, as a potential marker gene for the root cap. Strikingly, the expression of this gene was restricted to the outer central columella and LR cap cells (Kamiya et al., 2016). Nevertheless, the specificity of its expression within root tissues and during different developmental phases remained to be explored. To test its expression specificity, we fused the promoter of *At5g54370* to an *eGFP-GUS* fusion reporter and transformed the resulting construct into *Arabidopsis* to validate its cell-type-specific expression (Figure 1). GFP expression was restricted to the root-cap cells of homozygous 5-day-old *At5g54370 promoter:eGFP-GUS* plants (Figure 1). We observed no reporter gene expression in other developmental zones (i.e.,

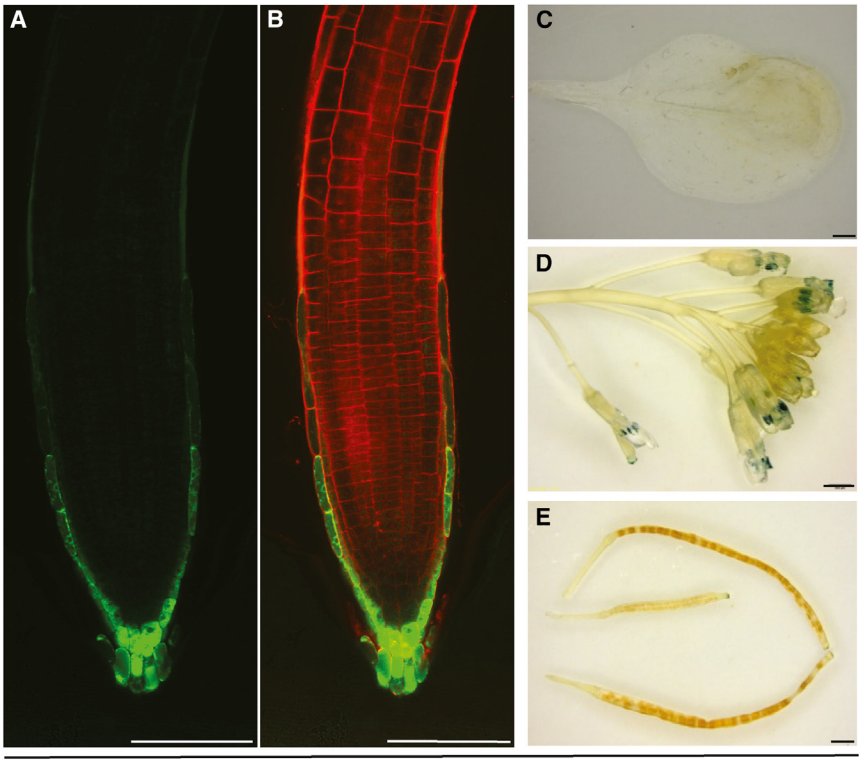

Figure 1. Identification and validation of an *Arabidopsis* root-cap cell-specific promoter
(A and B) Confocal microscopy of 5-day-old homozygous *pAt5g54370:eGFP-GUS* seedlings revealed a GFP signal exclusively in root-cap cells of the primary root.
(C–E) GUS histochemical analysis of leaves, flowers, and siliques revealed that, with the exception of anthers and stigmas, reporter gene expression was not visible at any other growth stages. Scale bars correspond to 100 μm **(A** and **B)** and 1 mm **(C–E)**.

the transition zone and differentiated zone) of PRs and LRs. Similarly, expression was not detected in vegetative tissues such as leaves and stems (Figure 1C). However, slight (low) reporter activity was detected in the anthers and stigma of closed flower buds (Figure 1D). We used this *At5g54370 promoter:eGFP-GUS* line to sort root-cap cells for further experiments.

To characterize spatiotemporal changes in the root-cap-specific proteome in response to salt treatment, we performed a root-cap-specific proteomic study using the *pAt5g54370:eGFP-GUS* line (supplemental Figure 1A). We performed liquid chromatography and a hybrid quadrupole orbitrap mass spectrometry run with protein extracts from root-cap and non-root-cap cells. We detected 304 and 440 proteins in the root-cap and non-root-cap cells, respectively, under control and salt-stress treatment together (supplemental Figure 1C and supplemental Table 1). After excluding common proteins between control and salt-stress conditions, root-cap cells alone had 131 proteins, and non-root-cap cells had 217 proteins with unique peptides (supplemental Figure 1B and 1C and supplemental Table 1). We categorized these proteins as differentially translated based on differences in their presence and abundance between salt-stressed and control conditions. A protein with a fold change (FC) $\geq$ 1.5 in abundance was considered to be upregulated, and a protein with a FC $\leq$ 0.5 was considered to be downregulated. Some proteins were translated only under salt stress and were categorized as condition-specific proteins. Proteins in these three categories—upregulated, downregulated, and condition-specific—were termed stress-responsive proteins (supplemental Figure 1B and 1C and supplemental Table 1B). More stress-responsive proteins were identified in root-cap cells (109) than in non-root-cap cells (79) (supplemental Figure 1C). This result suggests that root-cap cells may play a key role during the early events of salt perception and relay the signal to neighboring cell types.

The root cap is an active center during salt-stress signaling

We identified several salt-stress-responsive proteins in root-cap cells compared with non-root-cap cells (supplemental Figure 1C). To better understand the biological processes regulated by these salt-responsive proteins, we constructed a bipartite network consisting of the biological processes associated with each protein and its translation status in root-cap and non-root-cap cells upon salt stress (Figure 2 and supplemental Table 1D). Several salt-responsive proteins were translated or upregulated in root-cap cells, but most responsive proteins in non-root-cap cells were downregulated, indicating that the root cap is an active center during salt stress. Interestingly, within the root-cap cells, most salt-responsive proteins were upregulated or specifically translated at the 12-h time point but downregulated or absent at the 24-h time point (Figure 2). In general, when plants are under stress, they try to balance growth and development with stress defense and adaptation. During the initial stage of stress, plants attempt to briefly curtail growth by limiting energy-consuming processes like protein metabolism (translation, processing, synthesis, etc.) and instead spend the energy on construction of stress-response molecules used in the adaptation process (Ndimba et al., 2005). Here, many of the salt-responsive proteins identified in root-cap cells were associated with biological processes such as transcription, post-transcription, translation, and post-translational regulation. Numerous 40S and 60S ribosomal subunits, such as RPL4A, RPL4D, RPL9D, RPP0B, EMB2171, and At2g44210 of the 60S subunit and RPS4B, RPS9B, and RPS10B of the 40S subunit, were active (either upregulated or specifically present) in root-cap cells under salt stress at the 12-h time point compared with non-root-cap cells (Figure 2). We also observed many candidate proteins responsible for folding of *de novo* synthesized proteins in root-cap cells but not non-root-cap cells upon salt stress; these included the chaperone proteins HSC70-1, CPN10, and P23-1 (HSP90), along with CRT1 (Calreticulin-1) and At5g07340 (Calreticulin family) (Figure 2). This suggests that upon perception of salt stress by root-cap cells, protein translation and turnover are more active to manage the downstream activities of salt signaling. We next examined whether any known salt-stress

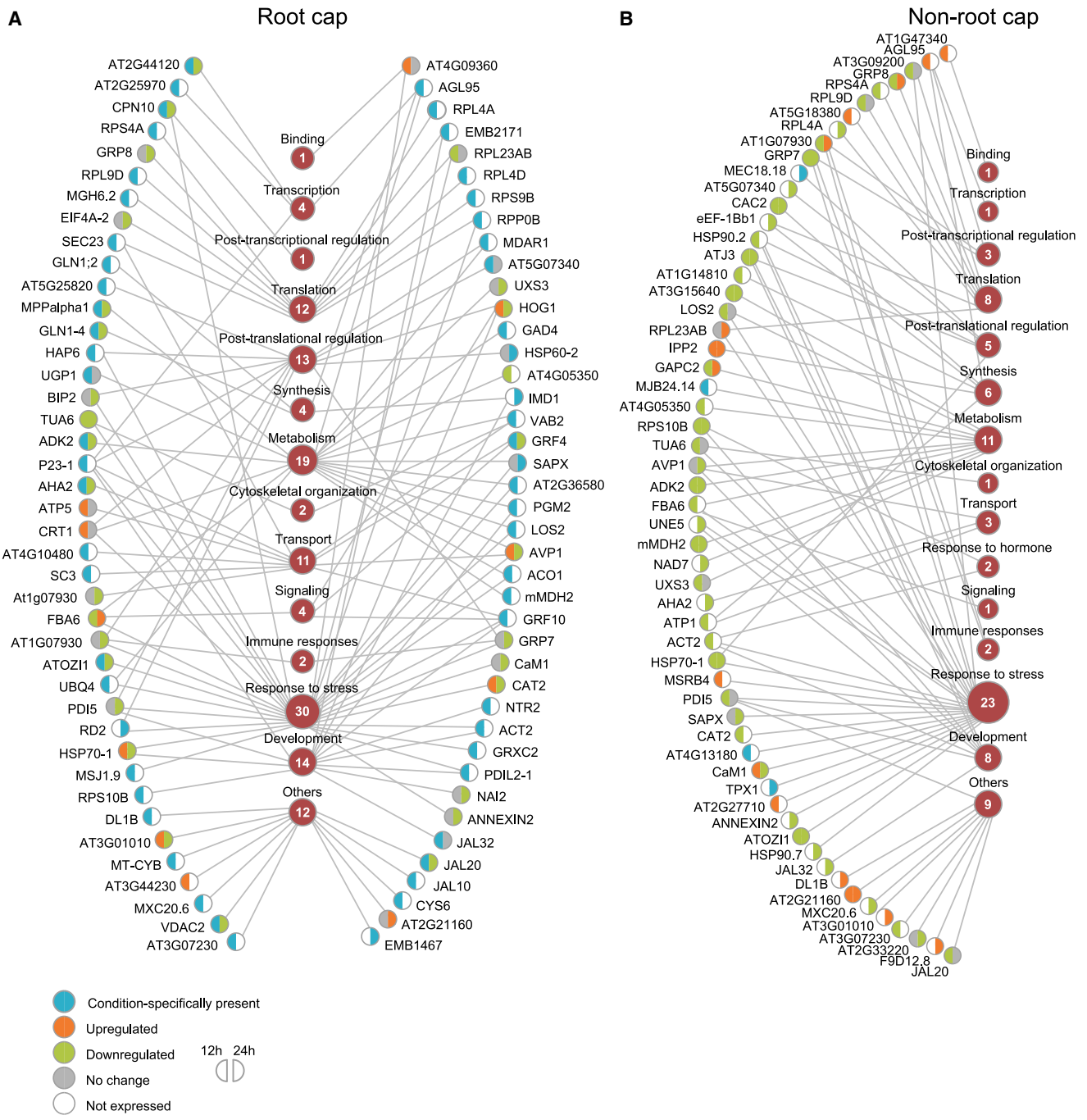

Figure 2. The root cap is an active center under salt stress compared with non-root-cap cell types

(A) Bipartite network of the translation status and associated biological processes of salt-stress-responsive proteins in **(A)** root-cap cells and **(B)** non-root-cap cell types. The biological processes (center of the figure) associated with a protein are connected via an edge. The number of proteins representing each biological process is given on the associated node. The protein's translation status and regulation at 12 and 24 h of salt treatment is given in the two halves of the node, with different colors based on the regulation, as mentioned at the bottom of the figure.

response proteins were translated specifically in root-cap cells upon salt stress.

Components of the salt signaling pathway operating in the root cap

Perception of salt stress evokes different signaling cascades, such as osmotic, ROS, ionic, and phytohormone signaling, to adapt or cope with salt stress. When salt stress is perceived at the root tip, Ca^{2+} waves travel from the perception site to distal shoot tissues via cortical and endodermal cells (Choi et al., 2014). We identified the presence of one such calcium sensor, the *Arabidopsis* calmodulin 1 (CaM1) protein, in both root-cap and non-root-cap cell types. Although the CaM1 translation level did not change in root-cap cells, it was upregulated in non-root-cap cells after 12 h of salt stress and downregulated

at 24 h (Figure 2). This spatiotemporal pattern of CaM1 translation in root-cap and non-root-cap cells could indicate spatial passing of the salt stress signal in the *Arabidopsis* root. Increased levels of Ca^{2+} activate NADPH oxidase, resulting in extracellular ROS production. Extracellular ROS lead to AtANNEXIN1 (AtANN1)-mediated Ca^{2+} influx, which in turn promotes transcription of the Na^+/H^+ antiporter SOS1 in root epidermal cells (Laohavisit et al., 2013). Here, we identified AtANN2 (ANNEXIN2), a close homolog of AtANN1, in root-cap cells at 12 h and found that it was downregulated after 24 h of salt treatment. We observed the active presence of two peroxisomal proteins, CAT2 and MDAR1, in root-cap cells under salt stress, but these proteins were downregulated or absent in non-root-cap cells (Figure 2). Both CAT2 and MDAR1 are known for their roles in ROS scavenging during salt stress (Eltayeb et al., 2007; Song et al., 2021).

Generation of proton-motive force across membranes by proton pumps such as H^+-ATPase and vacuolar H^+-pyrophosphatase is necessary to lower cytosolic Na^+ concentrations using Na^+/H^+ antiporters. We identified several proton pumps and voltage-dependent anion channels (VDACs) translated in root-cap cells during salt stress compared with non-root-cap cell types. For example, the plasma membrane (PM) H^+-ATPase AHA2, the vacuolar H^+-ATPase subunit VAB2, the vacuolar H^+-pyrophosphatase AVP1, and voltage-dependent anion channel 2 (VDAC2) were all condition-specifically translated in root-cap cells. By contrast, 12 h of salt treatment did not regulate their protein translation in non-root-cap cells (Figure 2). The upregulation and presence of AVP1 and VAB2 in root-cap cells suggest that root-cap cells maintain ion homeostasis by sequestering Na^+ in the vacuolar lumen (Gaxiola et al., 2002; Duan et al., 2007). At the same time, the proton gradient generated by AHA2 across the plasma membrane is required for exclusion of Na^+ from the cell by the SOS1 transporter. During this process, interaction with 14-3-3 proteins such as GENERAL REGULATORY FACTOR2 (GRF2) and GRF6 activates AHA2 and enhances the proton gradient across the plasma membrane (Fuglsang et al., 2007; Zhou et al., 2014; Yang et al., 2021). We found two other 14-3-3 proteins, GRF4 and GRF10, in root-cap cells upon salt stress that might participate in regulation of AHA2. Similarly, VDAC2, a mitochondrial outer membrane transport protein, was found specifically in root-cap cells and is known to positively regulate SOS2 and SOS1 during salt stress (Liu et al., 2015) (Figure 2). Together, these results suggest that root-cap cells are actively involved in Na^+ exclusion and sequestration during salt stress.

In addition to proteins with known roles in salt-stress response, we also observed some novel candidate proteins in root-cap cells compared with non-root-cap cells. Metabolite like γ-aminobutyric acid (GABA) content was increased in response to salt stress. GABA positively regulates salt tolerance by activating H^+-ATPase, SOS1, and NHX (Su et al., 2019). The key enzyme in the GABA shunt is glutamate decarboxylase (GAD), which synthesizes GABA from glutamate (Su et al., 2019). Another cellular enzyme, glutamine synthetase (GS or GLN) catalyzes the transformation of glutamate (Glu) into glutamine (Gln) and plays a crucial role in regulating ROS homeostasis under abiotic stresses like salt and cold (Ji et al., 2019). We found that glutamate decarboxylase 4 (GAD4), glutamine synthetase 1;2 (GLN1;2 or GSR2), and GLN1;4 were translated in root-cap cells upon salt stress but not in non-root-cap cells (Figure 2). We also noted the presence of three mannose-binding JALs—JAL10 (At1g52070), JAL20 (At2g25980), and JAL32 (At3g16440)—specifically in root-cap cells upon salt stress at the 12-h time point. These JALs were either downregulated or absent in non-root-cap cells upon salt stress. None of these JALs have previously been associated with salt-stress response in plants. However, a rice mannose-binding jacalin-related lectin (OsJRL) enhanced salinity tolerance in *Escherichia coli* and transgenic rice plants (He et al., 2017), and a barley jacalin-related lectin conferred salinity tolerance in *Saccharomyces cerevisiae* and *Arabidopsis* (Witzel et al., 2021). Thus, our root-cap-specific proteomics analysis revealed known and novel proteins involved in the early salt-response pathway of root cap cells.

Root-cap protein–protein interactome networks in response to salt stress

PPI networks were generated to visualize the salt-specific interactions among salt-responsive proteins in both root-cap and non-root-cap cell types compared with their respective control conditions. The PPI networks reveal condition-specific interactions in response to salt treatment over space and time and form major clusters (supplemental Figures 2 and 3). Under control conditions, very few interactions were observed in root-cap cells (supplemental Figure 2). However, 12 h after salt treatment, several proteins were condition-specifically translated and differentially accumulated compared with control conditions (supplemental Figures 2 and 3). In the case of non-root-cap cells under control conditions, several interactions were visualized among the identified proteins. However, these interactions were absent at 12 h of salt treatment, and several proteins were downregulated (supplemental Figures 2 and 3). A clear interaction among proteins involved in protein synthesis and turnover produced a significant cluster. Another cluster comprised proteins mainly involved in ER stress, probably owing to accumulation of misfolded/unfolded proteins (Figure 3). In response to abiotic and biotic stimuli, misfolded/unfolded proteins accumulate in the ER and cause ER stress. This ER stress is alleviated by initiation of the unfolded protein response (UPR) and ER-associated degradation (ERAD) of misfolded proteins. The activated UPR increases the expression of ER chaperones and ERAD components that aid in proper protein folding and degradation of unfolded proteins, respectively (Liu et al., 2011; Reyes-Impellizzeri and Moreno, 2021). Salt treatment induces the expression of ER chaperones such as luminal binding protein (BiP1/2), calreticulin (CRT), calnexin (CNX), and protein disulfide isomerase 5 (PDI5) (Liu et al., 2011; Zhang et al., 2021), which help to mitigate ER stress. In this study, 12 h after salt treatment, CRT1 (upregulated), BiP2, PDI5, and the ER body protein NAI2 were present in root-cap cells. All of these proteins were involved in condition-specific interactions with other molecular chaperones such as heat shock proteins (HSPs) and GRF10 and GRF4 (Figure 3). This condition-specific PPI was missing in non-root-cap cells (Figure 3). Three HSPs from the HSP90 family (HSP90.2, HSP90.7, and HSP81-2) and two members of the HSP70 family (HSP70-1 and HSP70-15) were also part of this cluster. These PPIs were not observed in non-root-cap cells under salt stress

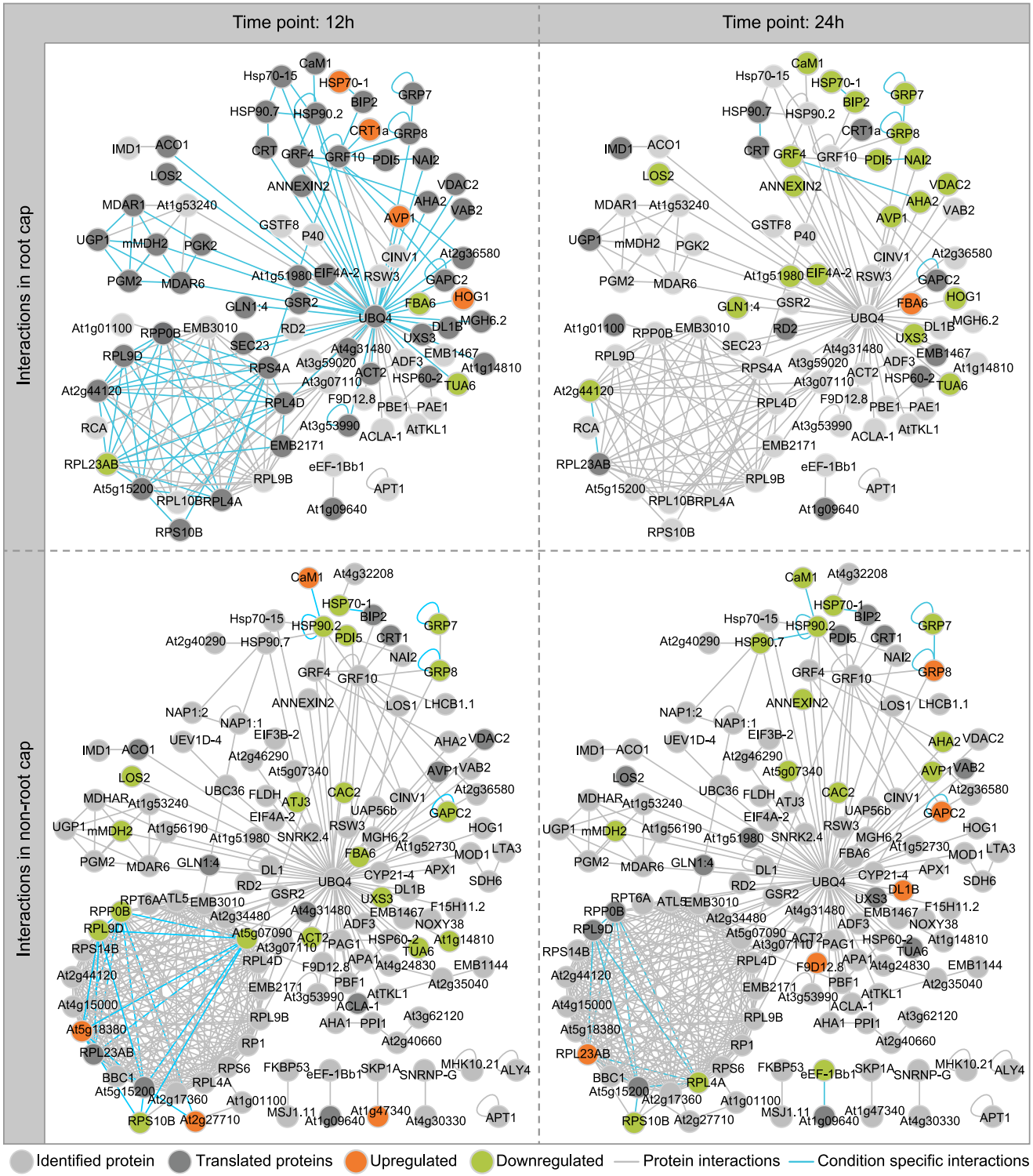

Figure 3. Interactome map of root-cap and non-root-cap cells under salt stress

The protein–protein interactome of proteins translated in both root-cap and non-root-cap cells was reconstructed using interactions from the BioGRID4.4 database. The proteins translated under salt-stress conditions are highlighted in different colors, as mentioned in the figure. The edge is blue if the interaction is possible in that particular condition and cell type as per its translation status from our proteomic study.

(Figure 3). All these PPI interactions in root-cap cells upon salt stress indicate that root-cap cells mitigate the negative effect of salt stress on growth by activating the ERAD and UPR signaling pathways.

We found another small PPI cluster comprising protein components involved in ROS scavenging and primary glycolytic enzymes (Figure 3). Monodehydroascorbate reductase 1 (MDAR1) and MDAR6 were translated in a condition-specific manner in

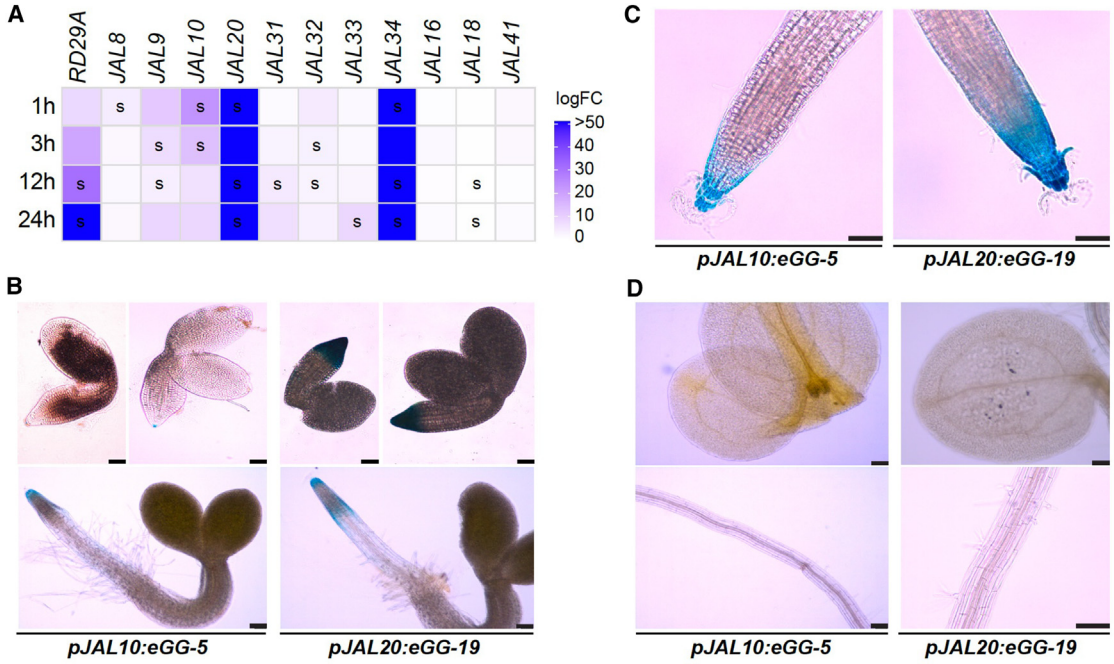

Figure 4. Jacalin-associated lectins as novel root-cap-specific salt-stress-responsive proteins

(A) Heatmap showing the relative transcript levels of novel salt-stress-responsive proteins identified from our root-cap proteomics analysis (*JAL10*, *JAL20*, and *JAL32*), along with their close root-specific homologous *JAL*s under 1, 3, 12, and 24 h of salt stress. The transcript level of *RD29A*, a well-known marker gene for abiotic stress response, was used as a positive control for salt stress. *UBQ4* was used as the internal reference gene for qRT–PCR analysis. Mock-treated Col-0 was used as the control, and its expression was set to 1. Two to three biological replicates were used in the experiment, each consisting of at least 150 seedlings. S denotes the statistical significance of transcript level compared with the control using Student's *t*-test. Refer the bar graph in supplemental Figure 4 for details.

(B–D) Root-cap-specific expression of *JAL10* and *JAL20*. GUS histochemical staining of *pJAL10:eGFP-GUS* and *pJAL20:eGFP-GUS* shows the radicle cell-specific expression of reporter gene during **(B)** seed germination from imbibition onward. After germination **(C and D)**, reporter gene expression is confined to root-cap cells in *pJAL10*, whereas in *pJAL20*, expression is also seen in some non-root-cap cell types. This pattern of GUS staining is also consistent with GFP reporter gene expression, as shown in supplemental Figure 5. Reporter gene expression was not observed in leaves or other root parts in either *promoter:reporter* line. The scale bars represent 25 μm **(A)** and 100 μm **(C and D)**.

root-cap cells. MDARs are known to participate in the ascorbate–glutathione cycle and in removal of toxic H_2O_2 (Eltayeb et al., 2007). A recent study of post-translational protein modifications in *Arabidopsis roots* under persistent osmotic and salt stress revealed the accumulation of lysine acetylation events in primary glycolytic enzymes such as UDP-glucose pyrophosphorylase 1, phosphoglycerate kinase 2, and ENOLASE 2 (Rodriguez et al., 2021). Consistent with this report, we also observed translation of pyrophosphorylase 1, phosphoglycerate kinase 2, and ENOLASE 2 in root-cap cells in response to salt treatment. The PPI network analysis thus revealed salt-responsive protein interactions that occurred specifically in root-cap cells compared with non-root-cap cells. The same PPIs were absent, or the proteins involved in the PPI were downregulated, after 24 h of salt treatment in root-cap cells.

JAL10—a salt-responsive root-cap-specific protein

After identifying ER stress components that formed a major PPI cluster in root-cap cells upon salt stress, we sought to identify the candidate proteins associated with this process. We selected three mannose-binding JALs—JAL10, JAL20, and JAL32—identified in root-cap cells for further study. The motivation for this choice was that one of the two homologous lectins, CRT and CNX, was specifically translated and upregulated in root-cap cells upon salt stress. CRT and CNX are known to work as molecular chaperones during folding and quality control in the ER (Caramelo and Parodi, 2008). The three selected JAL proteins were condition-specifically translated in root-cap cells 12 h after salt stress (Figure 2). However, JAL20 and JAL32 were downregulated in non-root-cap cells in the 12- and 24-h salt treatments, respectively. To date, there is no information on these proteins in the literature. Analysis of their expression profiles revealed that these three JAL proteins were exclusively coexpressed in the root-cap cells to various degrees (supplemental Figure 3). Quantification of their transcript levels revealed that these *JALs* were differentially expressed in response to salt treatment in a time-dependent manner (Figure 4A). The transcript level of *RD29A*, a known salt-responsive gene, was upregulated linearly up to 50-fold in a time-dependent manner after 24 h of salt treatment compared with control conditions (Figure 4A). The transcript profile of three JAL proteins (JAL10, JAL20, and JAL32) identified in the root-cap proteome showed the highest expression at 1 h of salt treatment, and their expression declined with increasing duration of salt exposure (Figure 4A). Following a 1-h exposure to salt treatment, the transcript levels of *JAL10*, *JAL20*, and *JAL32* increased 23-, 140-, and 4.5-fold compared with control conditions (Figure 4A and supplemental Figure 4). The increase in *JAL32* level was not significant at the 1-h time point but was significant (more than three-fold) at the 3-h time point (Figure 4A and supplemental

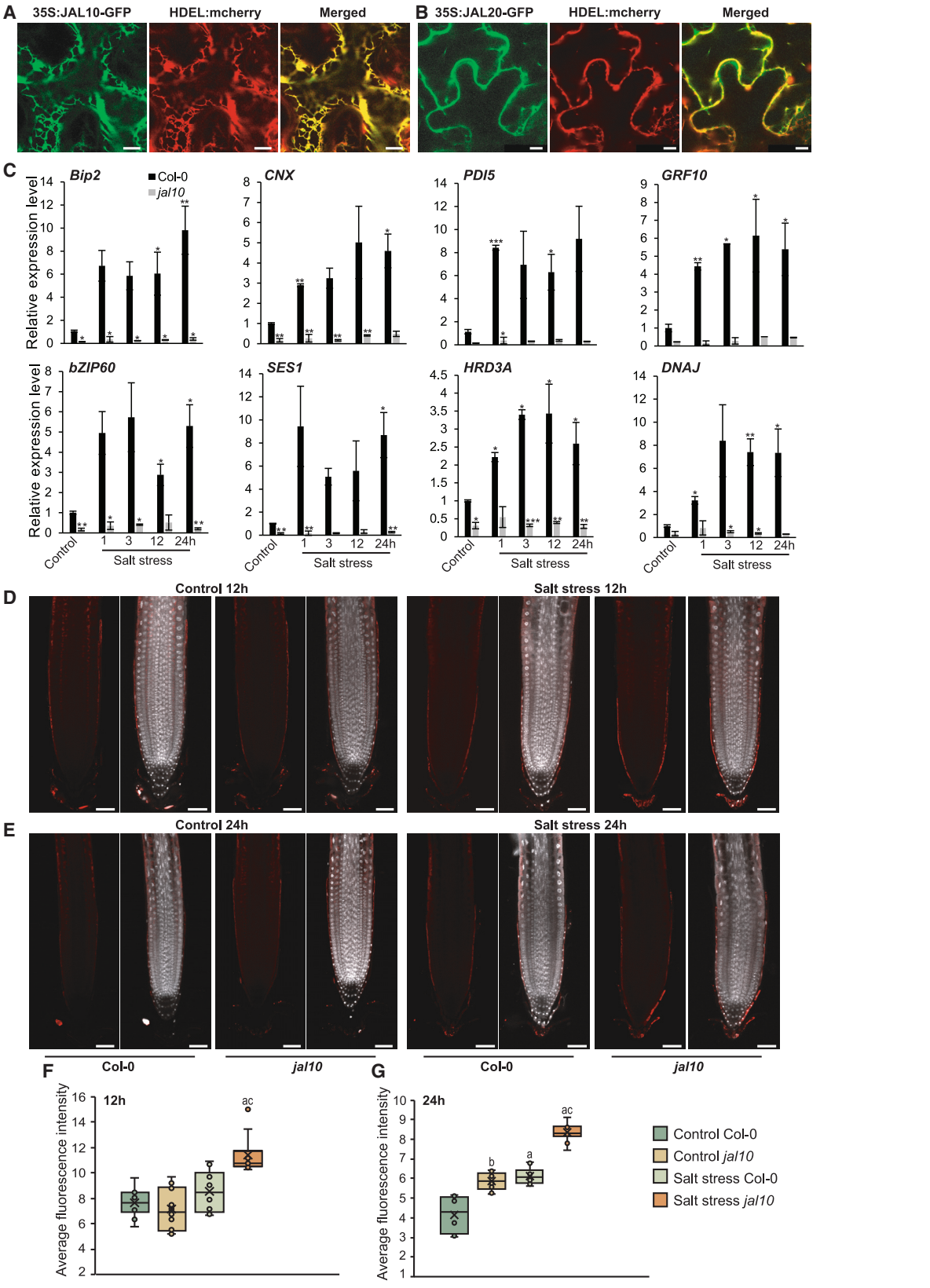

(legend on next page)

Figure 4). These observations indicate that *JAL10, JAL20, and JAL32* are involved in the early response to salt treatment. Their transcript profiles are consistent with our proteomics data, in which translation of the corresponding proteins was observed in root-cap cells at 12 h of salt treatment but was not observed or did not change after 24 h of treatment. Close homologs of *JAL10* (*JAL8*, *At1g52050*; and *JAL9*, *At1g52060*) and *JAL32* (*JAL31*, *At3g16430*; *JAL33*, *At3g16450*; and *JAL34*, *At3g16460*) also displayed increased expression in response to salt compared with the control. However, at early time points (1 and 3 h) post salt stress, there were no significant changes in the transcript levels of *JAL16* (*At1g60095*), *JAL18* (*At1g60130*), and *JAL41* (*At5g35940*), a close homolog of *JAL20*. However, the expression of *JAL18* was significantly reduced at later time points (12 and 24 h after salt treatment) in comparison with the control (Figure 4A and supplemental Figure 4). Our transcript analysis revealed the salt-stress specificity of the JALs reported to be coexpressed in the root cap. We next examined whether salt-responsive JAL proteins JAL10 and JAL20 were specifically expressed in the root cap. Homozygous transgenic plants containing *pJAL10*:*eGFP-GUS* and *pJAL20*:*eGFP-GUS* were generated to study the tissue-specific expression of the corresponding genes. *JAL10* reporter gene expression was confined to the root-cap cells from imbibition to germination and after germination (Figure 4B). By contrast, expression of the *JAL20* reporter gene was also apparent from imbibition onward, but its expression was visible throughout the entire root apical meristem, not only the root cap. After germination, expression of the *JAL10* and *JAL20* reporter genes was confined to the root-cap cells and apical meristem, respectively, and was not observed in other root cell types or leaves of 5-day-old seedlings (Figure 4C and 4D and supplemental Figure 5). Expression of *JAL10* and *JAL20* was consistent with the proteomics data, in which JAL10 was specifically translated in the root cap and JAL20 in root-cap and non-root-cap cells. These results show that salt stress leads to increased expression of some of the *JALs* in the root and that JAL10 is a salt-responsive, root-cap-specific protein.

JAL10 mediates the salt-stress-induced ER stress response

One of the prominent clusters in the PPI network of root-cap cells upon salt stress contained proteins involved in alleviation of ER stress. We therefore investigated whether the identified JAL proteins had a role in salt-mediated ER stress signaling. To participate in ER stress, these proteins must be located in or transported to the ER. To assess their localization, we created gene constructs in which *JAL10* and *JAL20* protein-coding sequences were fused to green fluorescent protein (*GFP*) and transiently expressed them in *Nicotiana benthamiana* leaves. Subcellular localization analysis revealed that both JAL10 and JAL20 were co-localized in the ER compartment together with the mCherry:HDEL marker (Figure 5A and 5B), but not with a plasma-membrane PIP2A:mCherry marker (supplemental Figure 6). Next, we examined whether JAL proteins had a role in regulating the ER stress pathway. To this end, we characterized the loss-of-function *jal10* mutant, as *JAL10* expression is specific to the root cap, whereas that of *JAL20* is not (Figure 4). Semi-quantitative RT–PCR of the *SALK_125442* T-DNA insertion line revealed that *jal10* is a null mutant (supplemental Figure 7). We then characterized the transcriptional regulation of ER-stress marker genes identified in the proteomics experiment (Figures 2 and 3) in the *jal10* mutant and the wild type under progressive salt-stress treatment (Figure 5C). Our proteomics analyses revealed that salt treatment resulted in translation of BiP2, CNX, PDI5, and GRF10 in root-cap cells. Consistent with the proteomics data, transcript levels of BiP2, CNX, PDI5, and GRF10 were upregulated in a time-dependent manner in the wild type (Figure 5C). Expression of these genes was reduced under control conditions in the *jal10 mutant* compared with the wild type. Surprisingly, and in contrast to its effects on the wild type, salt treatment did not evoke upregulation of these transcripts in *jal10* (Figure 5C). This result suggested that JAL10 function might be necessary for upregulation of these molecular chaperones.

We also examined the transcript levels of genes such as bZIP60, SENSITIVE TO SALT1 (SES1), and Hmg-CoA reductase degradation 3A (HRD3A), which are known to participate in the ER stress pathway. The bZIP60 transcription factor has been shown to be essential for UPR gene activation mediated by the ER stress sensor inositol-requiring enzyme 1 (IRE1) (Deng et al., 2011); SES1 is activated by another ER stress sensor, bZIP17, and acts as a molecular chaperone to mitigate salt-induced ER stress (Guan et al., 2018); and HRD3A is an active player in the ERAD pathway (Su et al., 2011). DNAJ3 encodes a molecular co-chaperone from the HSP40 family that is regulated by different abiotic stresses, including salt, and is important for seed development (Salas-Muñoz et al., 2016). Transcript levels of *bZIP60*,

Figure 5. The ER-localized JAL10 protein regulates ER stress-associated UPR gene expression and accumulation of misfolded proteins in response to salt stress

(A and B) Transient protein expression in *Nicotiana benthamiana* revealed that JAL10 and JAL20 were localized to the ER. Tobacco leaves infiltrated with C-terminal GFP-fusion proteins of **(A)** JAL10 and **(B)** JAL20 together with the HDEL:mCherry marker. Scale bars correspond to 10 μm **(A and B)**.
(C) The relative transcript levels of ER-associated UPR genes were attenuated in the *jal10* mutant background. qRT–PCR analysis was carried out in the Col-0 and *jal10* mutant background under control and high-salt treatments. Expression of identified ER-stress genes was quantified under high salt stress compared with the control. *UBQ4* was used as the internal reference gene. Mock-treated Col-0 was used as the control, and its expression was set to 1. Two to three biological replicates were used, each consisting of at least 150 seedlings. The statistical significance of transcript level compared with the control was calculated using Student's *t*-test. The values shown are mean ± SD. $^{*}p < 0.05$, $^{**}p < 0.01$, $^{***}p < 0.001$. Confocal microscopy images of Col-0 and *jal10* mutant plants under salt stress for **(D)** 12 h and **(E)** 24 h show increased accumulation of misfolded protein aggregates in root-cap cells of *jal10* mutant plants. The protein aggresomes (red) were stained with Proteostat aggresome detection dye, and nuclei were stained with Hoechst 33342 (pseudocolor gray). Scale bars correspond to 50 μm. The boxplots represent the average fluorescence intensity of Proteostat aggresome red dye in root-cap regions of Col-0 and *jal10* mutant plants under salt stress for **(F)** 12 h and **(G)** 24 h. The values shown are mean ± SD. The statistical significance of differences in fluorescence level was calculated using a two-way ANOVA (Bonferroni's post-test). "a" denotes significant differences ($p < 0.001$) between the control and salt treatments within a genotype. "b" denotes a significant difference between Col-0 and *jal10* under control conditions. "c" denotes a significant difference between Col-0 and *jal10* under salt treatment.

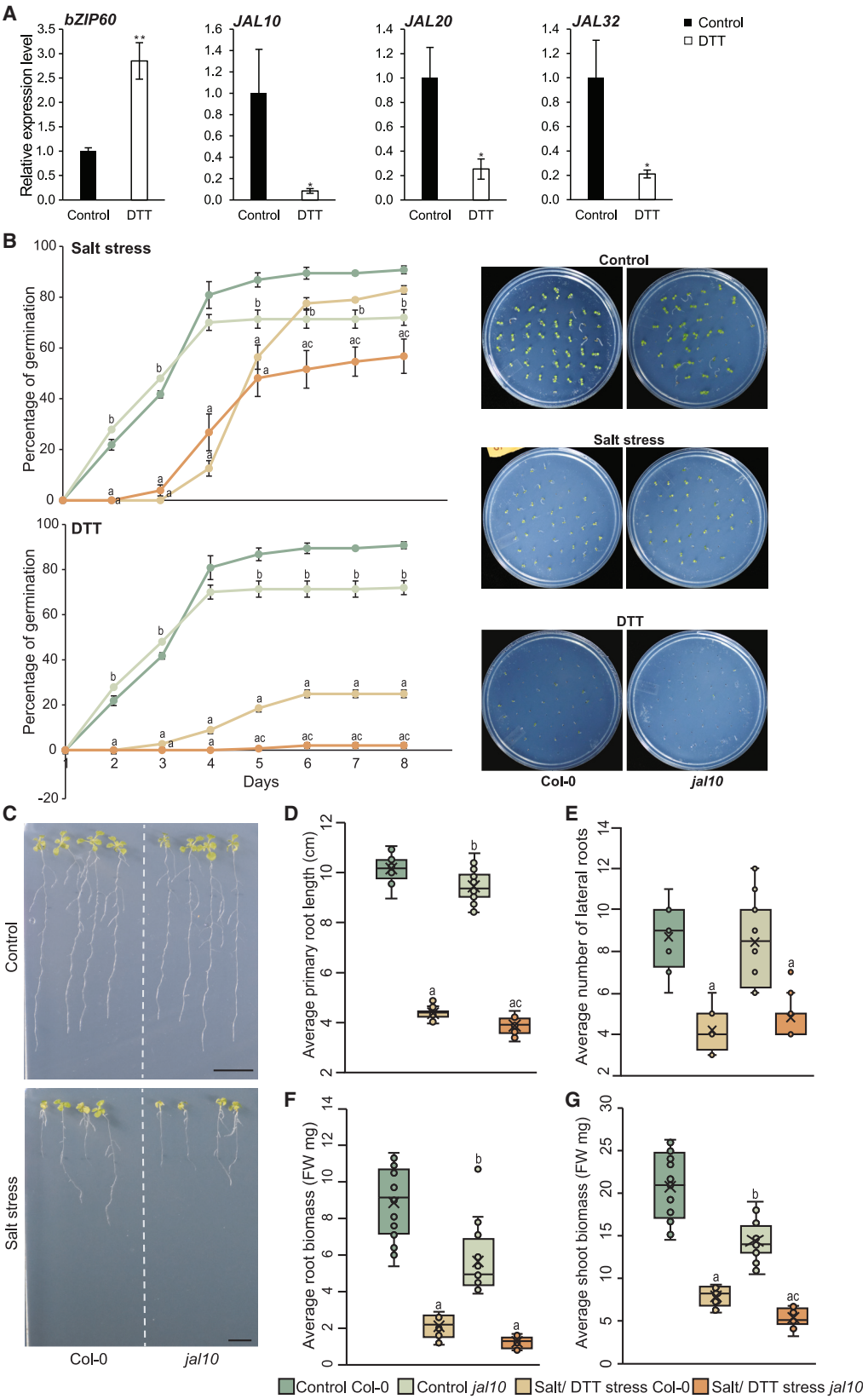

(legend on next page)

SES1, *HRD3A*, and *DNAJ* were significantly upregulated several fold in wild-type plants under salt stress compared with control conditions (Figure 5C). By contrast, their transcript levels were lower in the *jal10* mutant than in the wild type under control conditions, and salt treatment did not cause a significant increase in their transcript levels in *jal10* (Figure 5C). One of the main strategies by which cells alleviate ER stress is the accelerated degradation of misfolded proteins through ERAD. HRD3A is actively involved in regulating misfolded proteins during the ERAD process under salt stress (Liu and Howell, 2010; Liu et al., 2011; Su et al., 2011), and the *hrd3a* mutant displayed hypersensitivity to salt stress due to an increased misfolded protein response (Liu et al., 2011). Here, expression of HRD3A was attenuated in the *jal10* mutant in response to salt stress (Figure 5C). We therefore examined whether this attenuation of HRD3A led to increased aggregation of misfolded proteins in *jal10* compared with the wild type (Figure 5D and 5E). Using a commercially available aggresome detection kit (Proteostat aggresome detection kit, ENZO), we visualized the distribution of misfolded protein aggregates under salt stress. Salt stress and a known inducer of ER stress, MG132, caused aggregation of misfolded proteins in both Col-0 and the *jal10* mutant (Figure 5D–5F and supplemental Figure 8). When the proteasome inhibitor MG132 was used, levels of misfolded proteins in wild-type and *jal10* mutant seedlings increased by 61% and 75%, respectively, compared with those under control conditions (supplemental Figure S8). In response to salt treatment, the wild type exhibited increases of 12% and 48% in accumulation of protein aggresomes at 12 and 24 h, respectively. By contrast, *jal10* displayed increases of 59% and 42% at 12 and 24 h. In addition, the *jal10* mutant displayed significant increases of 33% and 36% in the aggregation of misfolded proteins in the 12- and 24-h salt stress treatments compared with the wild type (Figure 5F and 5G). Interestingly, misfolded aggregates were detected more in the root-cap region of the *jal10* mutant (Figure 5D and 5E). Together, these results suggest that JAL10 might be crucial for the salt-stress-mediated ER-stress pathway. In addition, it is plausible that JAL10 may participate in activation of many regulators implicated in salt-stress mitigation, perhaps through a mechanism that remains to be identified.

The *jal10* mutant displayed a hypersensitive response to salt stress

To test whether the role of JAL10 was specific to salt-mediated ER stress or a generic response to ER stress, wild-type plants were treated with dithiothreitol (DTT), which rapidly induces ER stress by blocking disulfide-bond formation (Je et al., 2022). As expected, expression of *bZIP60*, a known regulator of ER stress, was upregulated by ~2.7-fold in DTT-treated Col-0 seedlings compared with untreated controls (Figure 6A). By contrast, transcript levels of *JAL10*, *JAL20*, and *JAL32* were significantly downregulated by 75%–90% compared with control conditions. These results suggest that DTT-mediated ER stress has an inhibitory effect on *JAL* expression (Figure 6A). Because JAL10 is expressed from seed imbibition through seed germination, we examined whether the seed germination process was affected in the *jal10* mutant under control, salt-, and DTT-treated conditions (Figure 6B). Under control conditions, seed germination was significantly reduced in *jal10* mutant seeds compared with wild-type seeds. The wild type seeds showed ~90% germination after 4–5 days, but the *jal10 mutant seeds* showed approximately 70% germination, even after 8 days. Salt treatment caused a reduction of ~35% in the wild type 5 days after treatment, and germination of the wild type slowly increased with time. In the case of the *jal10* mutant, salt caused a similar reduction (32%) in germination at 5 days; however, it was not alleviated further as in the wild type, and *jal10* displayed a significant reduction in germination relative to the wild type at later time points under salt stress (Figure 6B). Furthermore, after DTT treatment, >90% reduction in germination percentage was observed in *jal10* mutant seeds compared with Col-0 seeds. These results suggest that JAL10 is a positive regulator of salt stress response during seed germination, and loss of *JAL10* function causes hypersensitivity of germination to salt stress. In response to DTT treatment, expression of *JALs* was reduced, and *jal10* mutant seeds had severe germination deficits.

We next investigated the effect of salt stress on *jal10* mutant growth and development after germination. The *jal10* mutant seedlings had significantly shorter PRs and fewer LRs under salt-stress conditions than under control conditions (Figure 6C–6E). Similar percentage reductions were observed in the wild type (Figure 6D and 6E): for example, salt-stressed PR length was reduced to 43% of control PR length in the wild type and to 41% of control PR length in *jal10*. However, the PR length of *jal10* mutant seedlings was significantly reduced by 12% compared with that of wild-type seedlings under salt stress. Under control conditions, *jal10* mutant seedlings had significantly lower shoot biomass (30% reduction) and root biomass (35% reduction) than wild-type seedlings. Salt stress caused similar reductions in the biomass of wild type (60% in shoots and 76% in

Figure 6. The *jal10* mutant is susceptible to salt and ER stress during germination and exhibits reduced growth under salt stress

(A) Relative transcript levels of *JAL10*, *JAL20*, and *JAL32* were lower under DTT-mediated ER stress. Mock-treated Col-0 was used as the control, and its expression was set to 1. *UBQ4* was used as the internal reference gene. Three biological replicates were used, each consisting of at least 150 seedlings. The statistical significance of transcript level compared with the control was determined using Student's *t*-test. $^{*}p < 0.05$, $^{**}p < 0.01$.

(B) The *jal10* mutant plants showed reduced seed germination under control, salt-stress, and DTT-stress treatments. Each plate contains approximately 50 seedlings ($n = 3$). The values shown are the mean ± SE.

(C) Growth of Col-0 and *jal10* mutant plants on control medium and salt-containing medium (150 mM NaCl) for 7 days. Scale bars correspond to 1 cm.

(D–G) Comparisons of **(D)** primary root length, **(E)** lateral root number, **(F)** root biomass, and **(G)** shoot biomass between Col-0 and *jal10* mutant plants under salt stress. The values shown are mean ± SD. The statistical significance in **(B** and **D–G)** was compared among genotypes and conditions using a two-way ANOVA followed by a Bonferroni's post-test. "a" denotes significant differences ($p < 0.05$) between the control and treatment within a genotype. "b" denotes a significant difference between Col-0 and *jal10* under control conditions. "c" denotes a significant difference between Col-0 and *jal10* under salt or DTT treatment. FW, fresh weight.

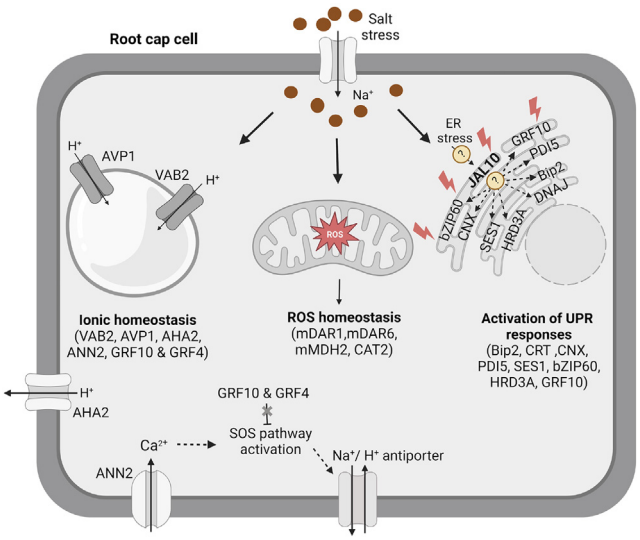

Figure 7. The root-cap-specific proteome in response to salt stress

The proteome and PPI analysis of root-cap cells under salt stress reveal several known and novel candidates participating in the salt adaptation of root-cap cell types. Several proton pumps associated with salt exclusion or sequestration are specifically translated to restore Na^+ homeostasis. Expression of several antioxidant proteins and other glycolytic enzymes deals with ROS production. Salt-stress-mediated ER stress triggers expression of JAL10 specifically in the ER, where it may participate in regulation of UPR gene expression directly or indirectly to restore protein homeostasis in the root-cap cell. It might be interesting to investigate how JAL10 regulates UPR gene expression in response to salt stress and how this regulation affects the size of ER bodies and the restoration of protein metabolism.

roots) and *jal10* mutant seedlings (64% in shoots and 78% in roots). However, the shoot biomass of *jal10* differed significantly from that of the wild type (Figure 6F and 6G). Together, these results suggest that the *jal10* mutant has reduced biomass and that salt stress significantly hampers its growth and development.

DISCUSSION

A chain of events occurs in a spatiotemporal manner when a plant cell is under salt stress, beginning with stress sensing and ending in either re-establishment of cellular ionic status or cell death, depending on the severity of the stress (Huh et al., 2002). However, it is not clear how Na^+ is sensed by plants, as there is no evidence of a putative channel or protein for the selective entry of Na^+ ions into the plant cell. Nevertheless, the downstream signaling cascade of salt sensing has been studied extensively (Knight et al., 1997; Liu et al., 2000; Qiu et al., 2004; Kim et al., 2007; Jiang et al., 2012). Cell-type-specific responses are crucial for fine-tuning environmental cues. Previous studies have highlighted the gene regulatory networks that operate in root cell types (e.g., pericycle, cortex, etc.) in response to high salt and iron deprivation (Dinneny et al., 2008; Geng et al., 2013). The initial perception of stress is crucial, as it determines the rest of the events and the fate of the plant under stress. Thus, it is interesting to investigate how the root cap, the first cell type to explore the rhizosphere region, perceives the salt-stress signal from the environment and relays it to the internal regulatory network and other root cell types. However, our understanding of cell-type-specific responses in the root cap is limited. This is because there has been no specific marker for both central columella and LR cap cells. PET111 (enhancer-trap line), which specifies only the central columella cells (Nawy et al., 2005; Brady et al., 2007; Dinneny et al., 2008; Petricka et al., 2012; Bargmann et al., 2013; Moussaieff et al., 2013), the M0028 GAL4-driver line, which specifies columella, LR cap, and epidermal tissues (Swarup et al., 2005; Petersson et al., 2009), and pGLABRA2 and the enhancer-trap line E4722 (Birnbaum et al., 2003; Gifford et al., 2008), which specify LR cap cells, have been used as marker lines. However, to our knowledge, no reporter line with specific expression both in central columella cells and LR cap cells has been used for root-cap-specific omics studies. The *At5g54370 promoter:eGFP-GUS* line generated in this study can be used to specifically sort root-cap cells for further downstream experiments (Figure 1). Here, we used this line to characterize the root-cap-specific proteome under control and high-salt conditions. The proteome landscape of the root cap consisted of 131 proteins, 11 of which were exclusively present in root-cap cells (supplemental Table 1C). JAL10 was among these 11 proteins, and its root-cap-specific expression was validated in the present study (supplemental Table 1 and Figures 2 and 4). Most of the remaining ten proteins have not yet been functionally characterized. Together with JAL10, these are important candidates whose roles in root-cap growth and development remain to be studied. A critical requirement for single-cell RNA-sequencing analysis is the availability of established marker genes for specific cell types. Thus, the proteins identified in this study can be used to identify root-cap cell types during single-cell RNA-sequencing analysis.

Our root-cap-specific proteomics study revealed the proteome landscape of root-cap cells under control and salt-stress conditions. Investigating the candidate proteins identified exclusively in root-cap cells will shed light on the growth and development of the root cap and its multifaceted role in the perception of environmental cues. Several proteins were either condition-specifically translated or upregulated in root-cap cells compared with non-root-cap cells, indicating that root-cap cells are an active center under salt stress (Figures 2 and 3). When we examined the protein landscape of the root cap under salt stress, it contained proteins from the canonical salt-signaling pathway that participate in the homeostasis of ions and ROS and the synthesis and turnover of proteins (Figure 7). For example, Na^+/H^+ antiporters are an integral part of the cell machinery that maintains Na^+ homeostasis, and their activities are regulated by the PMF generated by membrane-bound proton pumps. In the root cap, salt stress induced the translation of PM proton pumps such as AHA2 and 14-3-3 proteins such as GRF4 and GRF10. Homologs of the identified GRFs, GRF2 and GRF6, have been shown to inhibit SOS2 activity under normal conditions. They dissociate from SOS2 under salt stress, releasing it from inhibition and activating AHA2 to increase PMF across the PM (Fuglsang et al., 2007; Zhou et al., 2014; Yang et al., 2021). VDAC2, a mitochondrial outer membrane transport protein, is known to positively regulate SOS2 and SOS1 during salt stress (Liu et al., 2015). These proteins might be crucial for activating Na^+ exclusion mediated by the SOS pathway. We also observed condition-specific upregulation and presence of AVP1 and VAB2

in the root cap, both of which are known to participate in Na^+ sequestration in the vacuole. Overexpression of AVP1 has been shown to accelerate Na^+ sequestration in the vacuolar lumen, thereby increasing salt tolerance (Gaxiola et al., 2002; Duan et al., 2007) (Figures 2 and 7). The expression of ROS-scavenging enzymes such as CAT2 and the presence of MDAR1, MDAR6, mMDH2, and primary glycolytic enzymes also contribute to balancing ROS status and sustaining growth in root-cap cells under salt stress (Figures 3 and 7).

The PPI networks of stress-responsive proteins in root-cap and non-root-cap cells revealed that ER stress pathway components were translated and formed a major cluster in root-cap cells, but not non-root-cap cells, under salt stress (Figure 3). Recent studies have highlighted the role of ER homeostasis during salt stress. In response to salt stress, several ER-resident proteins, including chaperones such as BiP2, CRT, CNX, and PDI5, have been shown to be regulated at the transcriptional level (Liu et al., 2011; Zhang et al., 2021). CRT and CNX are critical for ER protein folding and Ca^{2+} homeostasis. Overexpression of wheat CRT proteins has been shown to enhance salt tolerance in tobacco (Xiang et al., 2015). In this study, CRT1 (upregulated), BiP2, PDI5, and the ER body protein NAI2 were translated in root-cap cells 12 h after salt treatment. These proteins are involved in condition-specific interactions with five other molecular chaperones, including HSPs. One of the HSPs, HSP90.7, is known to modulate the UPR by interacting with the ER-membrane-localized ribonuclease IRE1, which is a crucial player in UPR signal transduction (Marcu et al., 2002). All these ER-resident chaperones and HSPs might play crucial roles in protein processing in root-cap cells under salt stress (Figures 3 and 5). This study identified three JAL proteins that were translated in the root cap in response to salt. We characterized and validated one of these JALs, JAL10, which is localized to the ER and may be involved in regulation of the UPR response upon salt induction. Characterization of the *jal10* mutant revealed that UPR gene activation was attenuated, and increased accumulation of misfolded protein aggregates was observed in response to salt in root-cap cells of *jal10* compared with Col-0 (Figure 5D–5F and supplemental Figure S8). The *jal10* mutant displayed a hypersensitive response to salt in a seed germination assay, and reduced root growth and biomass were also observed (Figure 6). However, questions pertaining to the regulation of JAL10 and its role in UPR gene activation in response to salt require further investigation (Figure 7). Given that JAL10 is an ER-resident protein that encodes a mannose-binding lectin, it is tempting to speculate that it might also be involved in protein folding, similar to other lectin chaperones such as CNX/CRT. CNX/CRT participate in sequestration of nascent glycoproteins by recognizing N-linked oligosaccharides on glycoproteins (Caramelo and Parodi, 2008). On the other hand, homologs of the JAL proteins identified in our study, JAL30/PYK10 binding protein, JAL33, JAL34, and JAL35, are known to form a complex with PYK10/BGLU23, a beta-glucosidase. PYK10 and NAI2 are the two major ER body proteins, and JALs regulate ER body size by interacting with PYK10 and NAI2 (Nagano et al., 2008). ER bodies have been shown to play a role in plant responses to wounding, biotic stress, and abiotic stresses such as drought and metal ion toxicity (Li et al., 2022), and this might be another way in which JAL10 facilitates effective salt-stress response. The findings presented here pave the way for a better understanding of root-cap cell growth, development, and perception of environmental cues. Furthermore, they can facilitate the design of strategies to improve crop-plant salt tolerance and thus increase crop production under unfavorable conditions.

METHODS

Generation of promoter:reporter lines

The promoter region (942 bp upstream of the protein-coding sequence) of the late embryogenesis abundant protein-like gene (*At5g54370*) was amplified by PCR using *Arabidopsis* genomic DNA. The primers are listed in supplemental Table 2. The amplified promoter sequence was cloned into the pDONRP4-P1r plasmid (Invitrogen) using the GATEWAY BP reaction according to the manufacturer's protocol. The resulting pDONRP4-P1r-pAt5g54370 plasmid and an entry clone containing the reporter gene *eGFP-GUS* were shuttled into the binary vector pK7m24GW7 using a multisite GATEWAY LR reaction. Similarly, the promoter regions of *JAL10* (1226 bp upstream of ATG) and *JAL20* (938 bp upstream of ATG) were also cloned into the same vector and reporter combination to validate their root-cap-specific expression. All these constructs were transformed into the *Agrobacterium* strain GV3101 and then into *Arabidopsis* by the floral-dip method (Clough and Bent, 1998). Homozygous lines were identified in the T2 generation, and seeds of homozygous plants were used for further studies.

Plant material and growth conditions

We used T3 generation homozygous transgenic lines in all our experiments. For the root-cap-specific proteomics study, *pAt5g54370:eGFP-GUS* seeds were surface sterilized using a 5% sodium hypochlorite solution, then washed three times with double-distilled water. In the final step, 0.1% agarose was added to the seeds, and they were sown in a line on sterilized Nitex 03-250/47 mesh (Sefar America) placed onto $^1/_2$ MS plates (Murashige and Skoog [MS] medium, 1% sucrose, and 1% agar [pH 5.7]) for germination. The seedlings were grown in growth chambers under long-day conditions (16 h light/8 h dark, 150 μmol m^{-2} s^{-1} light intensity, 22°C day/20°C night, 65% relative humidity) for 5 days. For salt-stress experiments, 5-day-old seedlings were transferred to $^1/_2$ MS plates containing 150 mM NaCl and grown for 12 and 24 h. Three replicates were used for each condition (control, and 12 and 24 h). Approximately 24 000 seedlings (8000 per replicate) of the *pAt5g54370:eGFP-GUS* line for each condition were used to perform root-cap-specific proteomics. For the root growth assay and biomass estimation in response to salt stress, Col-0 and *jal10* were grown on $^1/_2$ MS plates for 3 days in a growth chamber. Later, they were transferred to medium containing 150 mM NaCl and grown for an additional 7 days before responses were observed. At the end of the 7th day, photos were taken, and PR length and LR number were determined using ImageJ software. Shoots and roots were separated and measured using a fine balance to estimate their fresh weights. For seed germination assays, 50 seeds each of Col-0 and *jal10* were placed onto $^1/_2$ MS plates containing 150 mM NaCl and 3 mM DTT. After 2 days of stratification, they were transferred to a growth chamber under long-day conditions, and germination was observed. The experiment was performed in three biological replicates.

Protoplast preparation

After the salt-stress treatment, root tips of the *pAt5g54370:eGFP-GUS* line were excised, and protoplasts were isolated as per Birnbaum et al. (2010). In brief, root tips (approximately 0.5 cm from the tip) were cut and immediately placed into protoplast solution (1.25% cellulase [Yakult], 0.3% macerozyme [Yakult], 0.4 M mannitol, 20 mM MES, 20 mM KCl, 10 mM $CaCl_2$, 0.1% BSA, 5 mM β-mercaptoethanol [pH 5.7]). The root tips were then cut into small pieces using a double-edged razor blade

(supplemental Figure 1), and the root tips and 30 ml protoplast solution were transferred to a 100-ml conical flask and placed in an incubator shaker (26°C) for 1 h and 45 min at 75 rpm. After incubation, the solution was passed through a 40-μm cell strainer to remove debris from the protoplasts. Protoplasts were then pelleted by centrifugation at 500 rpm for 10 min at room temperature. The supernatant was removed without disturbing the pellet. The pellet was resuspended in 500 μl protoplast buffer, and the quality of the isolated protoplasts was visualized using a binocular fluorescence microscope.

FACS sorting of GFP marker lines

Protoplasts from the control and salt-treated samples were sorted using a BD FACS Aria II instrument (BD Biosciences) at the flow cytometry facility of the Max Plank Institute for Molecular Genetics, Berlin, Germany. We used a 100-μm nozzle size and a sheath pressure of 20 psi for sorting. The voltage settings for measuring the scattering and emission of GFP signals were as described in Bargmann and Birnbaum (2010). The sorted GFP-positive and GFP-negative cells were collected into Eppendorf tubes containing RapiGest SF buffer (Waters) and immediately placed on dry ice. For the 12-h time point, approximately 37 000 GFP-positive cells per replicate were collected from the control samples, and 33 000 GFP-positive cells were collected from the salt-treated samples. The numbers of GFP-negative cells were approximately 100 000 from the controls and 41 000 from the salt-treated samples. The numbers of GFP-positive (control, 76 000 cells; salt, 22 500 cells) and GFP-negative cells (control, 357 000 cells; salt, 193 000 cells) for the 24 h-time point were different from those for the 12-h time point.

Protein extraction, digestion, and identification

Proteins were extracted from the sorted GFP-positive and GFP-negative cells using RapiGest SF (Waters, Eschborn, Germany, product code 186001860). The protoplasts were collected directly into 0.1% RapiGest SF (dissolved in 50 mM ammonium bicarbonate). In-solution digestion of whole protoplasts was performed following the manufacturer's instructions with some modifications. In brief, after sonicating the samples, we measured the protein concentrations using the Bradford assay (Kielkopf et al., 2020) and took equal concentrations in all samples. The samples were then treated with 2.5 mm DTT, and alkylation was performed with 7.5 mM 3-indole acetic acid. Trypsin digestion was performed in a 1:50 (weight to weight) ratio overnight at 37°C. The pH of the solution was adjusted to an acidic range to inactivate further activity of RapiGest SF, and peptides were concentrated using a vacuum centrifuge up to a 10-μl volume. Desalting was performed using Ziptips with 0.2 μl C18 resin (Merck Millipore, product code ZTC18M008) as per the manufacturer's protocol. The peptides were resuspended to a final concentration of 100 ng/μl using 2% acetonitrile and 0.1% trifluoroacetic acid. We used 6 μl of protein digest for nanoflow liquid chromatography on a Dionex UltiMate 3000 system (Thermo Scientific) coupled to a Q Extractive Plus mass spectrometer (Thermo Scientific) as described by Witzel and Matros (2020). Peptides were loaded onto a C18 trap column (0.3 × 5 mM, PepMap100 C18, 5 μm, Thermo Scientific) and then eluted onto an Acclaim PepMap 100 C18 column (0.075 × 250 mm, 2-μm particle size, 100-Å pore size, Thermo Scientific) at a flow rate of 300 nl min^{-1}. The mobile phases consisted of 0.1% formic acid (solvent A) and 0.1% formic acid in 80% ACN (solvent B). Peptides were separated chromatographically using a 100-min gradient from 2% to 44% solvent B, with the column temperature set to 40°C. A Nanospray Flex ion source was used for electrospray ionization of peptides, with a spray voltage of 1.80 kV, capillary temperature of 275°C, and S-lens RF level of 60. Mass spectra were acquired in positive-ion and data-dependent mode. Full-scan spectra (375–1500 m/z) were acquired at 140 000 resolution, and MS/MS scans (200–2000 m/z) were conducted at 17 500 resolution. The maximum ion injection time was 50 ms for both scan types. The 20 most intense MS ions were selected for collision-induced dissociation fragmentation. Singly charged ions and unassigned charge states were rejected, and the dynamic exclusion duration was set to 45 s. All samples were measured in triplicate. The raw files were processed using Proteome Discoverer v2.4 and the Sequest HT search engine (Thermo Scientific) with the *A. thaliana* dataset from the SwissProt database (as of January 2021). The false discovery rate was set to 0.01, corrected using the Benjamini–Hochberg method, for highly confident identifications. Further parameters for the database search were: peptide tolerance, 10 ppm; fragment ion tolerance, 0.02 Da; tryptic cleavage with a maximum of two missed cleavages; carbamidomethylation of cysteine as a fixed modification; and oxidation of methionine as a variable modification. The result lists were filtered for high-confidence peptides, and their signals were mapped across all LC–MS experiments and normalized to the total peptide amount as per the same LC–MS experiment. The summed abundance method was used to calculate protein abundance. A differential protein expression ratio between the control and salt-treated samples was generated after an ANOVA test. The resulting protein list was further filtered on the basis of the following criteria: included proteins identified by at least two peptides or by a minimum of one unique peptide representing a protein coverage of more than 8% (this was to include small proteins that give only a small number of tryptic peptides). Furthermore, only those peptides identified in a minimum of two out of three biological replicates were considered. Raw proteome data have been deposited at MassIVE (https://massive.ucsd.edu/ProteoSAFe/static/massive.jsp) under the dataset ID MSV000091171.

Categorizing identified proteins as stress-responsive proteins

After identifying proteins, we performed further categorization based on the presence or absence of proteins in each sample. The presence of a protein was considered only when it was present in two out of three technical replicates and two out of three biological replicates. We generated a Venn diagram (Venny 2.1, Oliveros, 2007) of the proteins identified in control and salt-stress conditions in a cell-type-specific manner (i.e., root-cap cells and non-root-cap cells) (supplemental Figure 1B). The intersection (control ∩ salt stress) of the Venn diagram represents the common proteins between the control and salt-stress conditions. Among these, proteins with an abundance ratio (salt stress/control) FC $\geq$ 1.5 were considered to be upregulated, and those with an abundance ratio FC $\leq$ 0.5 were considered to be downregulated. From these analyses, we categorized stress-responsive proteins as those (root-cap or non-root-cap cells) that were detected exclusively in samples from salt treatments (condition-specifically present) or that were significantly differentially accumulated in response to salinity.

A bipartite network of stress-responsive proteins in a cell-type-specific manner

We analyzed the biological processes represented by the stress-responsive proteins in both root-cap cells and non-root-cap cells. We first retrieved biological process annotations for all *A. thaliana* proteins from the AmiGO database (Gene Ontology as of December 2021) and then assigned GO terms to each stress-responsive protein using this information. We used Cytoscape to create a network based on the GO terms associated with each protein.

Generation of a cell-type-specific interactome network of stress-responsive proteins

To reconstruct interactome networks of the stress-responsive proteins in root-cap cells and non-root-cap cells, we superimposed the root-cap proteomics data onto the global PPIs among *A. thaliana* proteins cataloged in the BioGRID4.4 database (as of December 2021). In brief, we retrieved the PPIs among all *Arabidopsis* proteins from the BioGRID4.4 database (https://thebiogrid.org). Here, we considered only experimentally proven interactions. A PPI can occur only when the two interacting proteins are present concurrently within a specific cell type under specific conditions. Using this criteria, we checked whether any of these proven interactions were possible among the identified proteins in root-cap and non-root-cap cells under a particular condition. A total of four PPI networks were created using Cytoscape v.3.10.0 (http://www.cytoscape.

org/) with respect to condition (control and salt stress) and cell type (root-cap and non-root-cap cells).

Histochemical analysis

Histochemical analysis of GUS (β-glucuronidase) activity was performed for *pAt5g54370*:*eGFP-GUS*, *pAt1g52070*:*eGFP-GUS*, and *pAt2-g25980*:*eGFP-GUS* at specific developmental stages from imbibition to 5 days after germination (DAG). GUS staining was performed as per Jefferson et al. (1987). After samples were placed in ice-cold acetone for one hour, 100 mM phosphate buffer (100 mM NaH_2PO_4, 100 mM Na_2HPO_4 [pH 7.4]) treatment was given. The samples were then immersed in staining solution (100 mM phosphate buffer, 50 mM $K_3Fe(CN)_6$, 50 mM $K_4Fe(CN)_6$, 0.015% X-Gluc, and 1% Triton X-100), vacuum infiltrated for 2 min, and incubated for 30 min at 37°C. They were cleared and mounted according to Malamy and Benfey (1997), and images were taken using a Leica DM 2000 LED microscope.

Subcellular localization of JAL proteins

The full-length coding sequences (CDSs) of *JAL10* (948 bp) and *JAL20* (1350 bp) without stop codons were amplified using cDNA and cloned into the pDONR221 plasmid (Invitrogen). This entry clone (pDONR221_CDS) and the destination vector pK7FWG2-GFP were used in an LR reaction to construct a CDS sequence with a C-terminal GFP tag. The resulting plasmid (pK7FWG2_CDS-GFP) was transformed into *Agrobacterium* strain GV3101. For subcellular localization studies, these vectors were co-transformed into *N. benthamiana leaves* together with an mCherry marker targeted to the PM or ER as described in Xu et al. (2015). Confocal images of infiltrated *N. benthamiana* leaves were taken after 72 h using a Leica SP8 microscope. GFP was excited at 488 nm, and emission was observed between 500 and 530 nm. mCherry was excited at 561 nm, and emission was observed between 600 and 680 nm.

Detection of aggregated misfolded proteins

Col-0 and *jal10* were grown on ½ MS plates for 5 days in a growth chamber, then transferred to medium containing 150 mM NaCl and grown for 12 and 24 h. Protein aggresomes were measured in roots using a Proteostat Aggresome Detection Kit (Enzo: ENZ-51035) according to the manufacturer's protocol with slight modifications. In brief, after salt treatment, at least 10 plants each of Col-0 and *jal10* were immediately fixed in 4% formaldehyde, then washed with 1× PBS. The seedlings were treated with permeabilization solution (0.5% Triton X-100, 3 mM EDTA [pH 8.0] and 1× assay buffer) for 30 min at 4°C and washed three times with 1× PBS. They were then incubated with PROTEOSTAT Aggresome Detection Reagent and Hoechst 33342 Nuclear stain (1:5000 dilution) in 1× PBS for 1 h at room temperature, washed with 1× PBS, and immediately imaged using a Leica SP8 confocal microscope. The Proteostat Aggresome detection red dye was excited with a 488-nm laser, and its emission was recorded between 500 and 620 nm. Hoechst 33342 nuclear stain was used to visualize nuclei; a 405-nm laser was used for excitation, and emission was recorded between 420 and 480 nm and represented in a grayscale pseudocolor. After imaging, signal intensity was measured by selecting only the root-cap region using Leica LASX software.

RNA isolation and qRT–PCR analysis

To measure transcript levels of candidate genes under salt stress, 5-day-old seedlings of Col-0 and the *jal10* mutant were treated with 150 mM NaCl for 1, 3, 12, and 24 h. For ER stress, 5-day-old Col-0 and *jal10 seedlings were treated with* 10 mM DTT for 6 h. After treatment, total RNA was extracted from whole roots using the TRIzol method. RNA was purified using a Nucleospin RNA Clean-up kit (MACHEREY-NAGEL, product code 740948.50). Genomic DNA was removed by treatment with DNAse I (Thermo Fisher Scientific). One microgram of cDNA was synthesized using the iScript Select cDNA synthesis kit (Bio-Rad, product code 1708897) with oligo(dT) primers. The cDNA samples were used to determine transcript levels by qRT–PCR as described in Ramireddy et al. (2018). The experiment was performed in two to three biological replicates (n = 150 seedlings per replicate). The primers used are listed in supplemental Table 2.

Statistical analysis

All qRT–PCR data in this publication were statistically analyzed using Student's t-test. The statistical significance of the proteostat aggresome, seed germination, and root physiology assays was computed by two-way ANOVA followed by Bonferroni's post-hoc test with non-normalized values.

DATA AND CODE AVAILABILITY

All data supporting the findings of this study are available within the paper and its supplementary data. Proteome raw data have been deposited at MassIVE (https://massive.ucsd.edu/ProteoSAFe/static/massive.jsp) under the dataset ID MSV000091171.

SUPPLEMENTAL INFORMATION

Supplemental information is available at *Plant Communications Online*.

FUNDING

This work was supported by IISER Tirupati and by an Early Career Research award from the Science and Engineering Research Board, Department of Science and Technology, Govt. of India (ECR/2016/001071) to E.R. K.K.D. acknowledges the CSIR-JRF fellowship and Bi-nationally supervised doctoral degree scholarship from DAAD (91730390) for her PhD. A.M. and A.P.G. acknowledge funding from IISER Tirupati for graduate studies. S.C. acknowledges funding from IISER Tirupati and the Ramalingaswami Re-entry Fellowship (BT/RLF/Re-entry/05/2018) Department of Biotechnology, Government of India.

AUTHOR CONTRIBUTIONS

K.W. and E.R. conceived the project, acquired the funding, and supervised the study. K.K.D. performed and analyzed most of the experiments. A.P.G. performed subcellular localization of JALs and detection of protein aggresomes. A.M. and S.C. contributed to data analysis, visualization of proteomics data, and construction of PPI networks. K.K.D. and E.R. wrote the original draft, and all authors reviewed, edited, and accepted the final version.

ACKNOWLEDGMENTS

E.R. kindly acknowledges the support extended by Prof. Thomas Schmülling, Freie Universität Berlin, while working in his lab during the generation of the root-cap-specific promoter:reporter line. We acknowledge the support provided by the flow cytometry facility of the Max Planck Institute for Molecular Genetics, Germany. The authors have no conflicts to declare.

Received: April 12, 2023
Revised: August 18, 2023
Accepted: September 27, 2023
Published: October 2, 2023

REFERENCES

Bargmann, B.O.R., and Birnbaum, K.D. (2010). Fluorescence activated cell sorting of plant protoplasts. J. Vis. Exp. 1673. https://doi.org/10.3791/1673.

Bargmann, B.O.R., Vanneste, S., Krouk, G., Nawy, T., Efroni, I., Shani, E., Choe, G., Friml, J., Bergmann, D.C., Estelle, M., et al. (2013). A map of cell type-specific auxin responses. Mol. Syst. Biol. **9**:688. https://doi.org/10.1038/msb.2013.40.

Batelli, G., Verslues, P.E., Agius, F., Qiu, Q., Fujii, H., Pan, S., Schumaker, K.S., Grillo, S., and Zhu, J.K. (2007). SOS2 promotes salt tolerance in part by interacting with the vacuolar H+-ATPase and

upregulating its transport activity. Mol. Cell Biol. **27**:7781–7790. https://doi.org/10.1128/MCB.00430-07.

Birnbaum, K., Shasha, D.E., Wang, J.Y., Jung, J.W., Lambert, G.M., Galbraith, D.W., and Benfey, P.N. (2003). A gene expression map of the Arabidopsis root. Science **302**:1956–1960. https://doi.org/10.1126/science.1090022.

Bogoutdinova, L.R., Baranova, E.N., Baranova, G.B., Kononenko, N.V., Lazareva, E.M., Smirnova, E.A., and Khaliluev, M.R. (2020). Morpho-biological and cytological characterization of tomato roots (*Solanum lycopersicum* L., cv. *Rekordsmen*) regenerated under NaCl salinity *in vitro*. Cell tissue biol. **14**:228–242. https://doi.org/10.1134/S1990519X20030025.

Brady, S.M., Orlando, D.A., Lee, J.Y., Wang, J.Y., Koch, J., Dinneny, J.R., Mace, D., Ohler, U., and Benfey, P.N. (2007). A high-resolution root spatiotemporal map reveals dominant expression patterns. Science **318**:801–806. https://doi.org/10.1126/science.1146265.

Caramelo, J.J., and Parodi, A.J. (2008). Getting in and out from calnexin/calreticulin cycles. J. Biol. Chem. **283**:10221–10225. https://doi.org/10.1074/jbc.R700048200.

Choi, W.G., Toyota, M., Kim, S.H., Hilleary, R., and Gilroy, S. (2014). Salt stress-induced Ca2+ waves are associated with rapid, long-distance root-to-shoot signaling in plants. Proc. Natl. Acad. Sci. USA **111**:6497–6502. https://doi.org/10.1073/pnas.1319955111.

Clough, S.J., and Bent, A.F. (1998). Floral dip: a simplified method for *Agrobacterium*-mediated transformation of *Arabidopsis thaliana*. Plant J. **16**:735–743. https://doi.org/10.1046/j.1365-313x.1998.00343.x.

Deng, Y., Humbert, S., Liu, J.X., Srivastava, R., Rothstein, S.J., and Howell, S.H. (2011). Heat induces the splicing by IRE1 of a mRNA encoding a transcription factor involved in the unfolded protein response in Arabidopsis. Proc. Natl. Acad. Sci. USA **108**:7247–7252. https://doi.org/10.1073/pnas.1102117108.

Dinneny, J.R., Long, T.A., Wang, J.Y., Jung, J.W., Mace, D., Pointer, S., Barron, C., Brady, S.M., Schiefelbein, J., and Benfey, P.N. (2008). Cell identity mediates the response of Arabidopsis roots to abiotic stress. Science **320**:942–945. https://doi.org/10.1126/science.1153795.

Di Mambro, R., Svolacchia, N., Dello Ioio, R., Pierdonati, E., Salvi, E., Pedrazzini, E., Vitale, A., Perilli, S., Sozzani, R., Benfey, P.N., et al. (2019). The lateral root cap acts as an auxin sink that controls meristem size. Curr. Biol. **29**:1199–1205.e4. https://doi.org/10.1016/j.cub.2019.02.022.

Duan, X.G., Yang, A.F., Gao, F., Zhang, S.L., and Zhang, J.R. (2007). Heterologous expression of vacuolar H(+)-PPase enhances the electrochemical gradient across the vacuolar membrane and improves tobacco cell salt tolerance. Protoplasma **232**:87–95. https://doi.org/10.1007/s00709-007-0268-5.

Eltayeb, A.E., Kawano, N., Badawi, G.H., Kaminaka, H., Sanekata, T., Shibahara, T., Inanaga, S., and Tanaka, K. (2007). Overexpression of monodehydroascorbate reductase in transgenic tobacco confers enhanced tolerance to ozone, salt and polyethylene glycol stresses. Planta **225**:1255–1264. https://doi.org/10.1007/s00425-006-0417-7.

Essah, P.A., Davenport, R., and Tester, M. (2003). Sodium influx and accumulation in Arabidopsis. Plant Physiol. **133**:307–318. https://doi.org/10.1104/pp.103.022178.

Fu, H., and Yang, Y. (2023). How plants tolerate salt stress. Curr. Issues Mol. Biol. **45**:5914–5934. https://doi.org/10.3390/cimb45070374.

Fuglsang, A.T., Guo, Y., Cuin, T.A., Qiu, Q., Song, C., Kristiansen, K.A., Bych, K., Schulz, A., Shabala, S., Schumaker, K.S., et al. (2007). Arabidopsis protein kinase PKS5 inhibits the plasma membrane H+-ATPase by preventing interaction with 14-3-3 protein. Plant Cell **19**:1617–1634. https://doi.org/10.1105/tpc.105.035626.

Ganesh, A., Shukla, V., Mohapatra, A., George, A.P., Bhukya, D.P.N., Das, K.K., Kola, V.S.R., Suresh, A., and Ramireddy, E. (2022). Root Cap to Soil Interface: A Driving Force Toward Plant Adaptation and Development. Plant Cell Physiol. **63**:1038–1051. https://doi.org/10.1093/pcp/pcac078.

Gaxiola, R.A., Fink, G.R., and Hirschi, K.D. (2002). Genetic manipulation of vacuolar proton pumps and transporters. Plant Physiol. **129**:967–973. https://doi.org/10.1104/pp.020009.

Geng, Y., Wu, R., Wee, C.W., Xie, F., Wei, X., Chan, P.M.Y., Tham, C., Duan, L., and Dinneny, J.R. (2013). A spatio-temporal understanding of growth regulation during the salt stress response in Arabidopsis. Plant Cell **25**:2132–2154. https://doi.org/10.1105/tpc.113.112896.

Gifford, M.L., Dean, A., Gutierrez, R.A., Coruzzi, G.M., and Birnbaum, K.D. (2008). Cell-specific nitrogen responses mediate developmental plasticity. Proc. Natl. Acad. Sci. USA **105**:803–808. https://doi.org/10.1073/pnas.0709559105.

Guan, P., Wang, J., Li, H., Xie, C., Zhang, S., Wu, C., Yang, G., Yan, K., Huang, J., and Zheng, C. (2018). SENSITIVE TO SALT1, An Endoplasmic Reticulum-Localized Chaperone, Positively Regulates Salt Resistance. Plant Physiol. **178**:1390–1405. https://doi.org/10.1104/pp.18.00840.

Guo, Y., Halfter, U., Ishitani, M., and Zhu, J.K. (2001). Molecular characterization of functional domains in the protein kinase SOS2 that is required for plant salt tolerance. Plant Cell **13**:1383–1400. https://doi.org/10.1105/tpc.13.6.1383.

He, X., Li, L., Xu, H., Xi, J., Cao, X., Xu, H., Rong, S., Dong, Y., Wang, C., Chen, R., et al. (2017). A rice jacalin-related mannose-binding lectin gene, OsJRL, enhances *Escherichia coli* viability under high salinity stress and improves salinity tolerance of rice. Plant Biol. **19**:257–267. https://doi.org/10.1111/plb.12514.

Hruz, T., Laule, O., Szabo, G., et al. (2008). Genevestigator v3: a reference expression database for the meta-analysis of transcriptomes. Adv. Bioinformatics. **420747**. https://doi.org/10.1155/2008/420747.

Huh, G.H., Damsz, B., Matsumoto, T.K., Reddy, M.P., Rus, A.M., Ibeas, J.I., Narasimhan, M.L., Bressan, R.A., and Hasegawa, P.M. (2002). Salt causes ion disequilibrium-induced programmed cell death in yeast and plants. Plant J. **29**:649–659. https://doi.org/10.1046/j.0960-7412.2001.01247.x.

Ismail, A., Takeda, S., and Nick, P. (2014). Life and death under salt stress: same players, different timing? J. Exp. Bot. **65**:2963–2979. https://doi.org/10.1093/jxb/eru159.

Je, S., Lee, Y., and Yamaoka, Y. (2022). Effect of common ER stress-inducing drugs on the growth and lipid phenotypes of Chlamydomonas and Arabidopsis. Plant Cell Physiol., pcac154 https://doi.org/10.1093/pcp/pcac154.

Jefferson, R.A., Kavanagh, T.A., and Bevan, M.W. (1987). GUS fusions: beta-glucuronidase as a sensitive and versatile gene fusion marker in higher plants. EMBO J. **6**:3901–3907. https://doi.org/10.1002/j.1460-2075.1987.tb02730.x.

Ji, Y., Li, Q., Liu, G., Selvaraj, G., Zheng, Z., Zou, J., and Wei, Y. (2019). Roles of cytosolic Glutamine synthetases in Arabidopsis development and stress responses. Plant Cell Physiol. **60**:657–671. https://doi.org/10.1093/pcp/pcy235.

Jiang, C., Belfield, E.J., Mithani, A., Visscher, A., Ragoussis, J., Mott, R., Smith, J.A.C., and Harberd, N.P. (2012). ROS-mediated vascular homeostatic control of root-to-shoot soil Na delivery in Arabidopsis. EMBO J. **31**:4359–4370. https://doi.org/10.1038/emboj.2012.273.

Kamiya, M., Higashio, S.Y., Isomoto, A., et al. (2016). Control of root cap maturation and cell detachment by BEARSKIN transcription factors in Arabidopsis. Development **143**:4063–4072. https://doi.org/10.1242/dev.142331.

Kanno, S., Arrighi, J.F., Chiarenza, S., Bayle, V., Berthomé, R., Péret, B., Javot, H., Delannoy, E., Marin, E., Nakanishi, T.M., et al. (2016). A novel role for the root cap in phosphate uptake and homeostasis. Elife **5**, e14577. https://doi.org/10.7554/eLife.14577.

Kielkopf, C.L., Bauer, W., and Urbatsch, I.L. (2020). Methods for measuring the concentrations of proteins. Cold Spring Harb. Protoc. **4**:102277. https://doi.org/10.1101/pdb.top102277.

Kim, B.G., Waadt, R., Cheong, Y.H., Pandey, G.K., Dominguez-Solis, J.R., Schültke, S., Lee, S.C., Kudla, J., and Luan, S. (2007). The calcium sensor CBL10 mediates salt tolerance by regulating ion homeostasis in Arabidopsis. Plant J. **52**:473–484. https://doi.org/10.1111/j.1365-313X.2007.03249.x.

Knight, H., Trewavas, A.J., and Knight, M.R. (1997). Calcium signalling in Arabidopsis thaliana responding to drought and salinity. Plant J. **12**:1067–1078. https://doi.org/10.1046/j.1365-313x.1997.12051067.x.

Kumpf, R.P., and Nowack, M.K. (2015). The root cap: a short story of life and death. J. Exp. Bot. **66**:5651–5662. https://doi.org/10.1093/jxb/erv295.

Laohavisit, A., Richards, S.L., Shabala, L., Chen, C., Colaço, R.D.D.R., Swarbreck, S.M., Shaw, E., Dark, A., Shabala, S., Shang, Z., et al. (2013). Salinity-induced calcium signaling and root adaptation in Arabidopsis require the calcium regulatory protein annexin1. Plant Physiol. **163**:253–262. https://doi.org/10.1104/pp.113.217810.

Liu, J.-X., and Howell, S.H. (2010). Endoplasmic reticulum protein quality control and its relationship to environmental stress responses in plants. Plant Cell **22**:2930–2942. https://doi.org/10.1105/tpc.110.078154.

Li, X., Li, X., Fan, B., Zhu, C., and Chen, Z. (2022). Specialized endoplasmic reticulum-derived vesicles in plants: Functional diversity, evolution, and biotechnological exploitation. J. Integr. Plant Biol. **64**:821–835. https://doi.org/10.1111/jipb.13233.

Lin, H., Yang, Y., Quan, R., Mendoza, I., Wu, Y., Du, W., Zhao, S., Schumaker, K.S., Pardo, J.M., and Guo, Y. (2009). Phosphorylation of SOS3-LIKE CALCIUM BINDING PROTEIN8 by SOS2 protein kinase stabilizes their protein complex and regulates salt tolerance in Arabidopsis. Plant Cell **21**:1607–1619. https://doi.org/10.1105/tpc.109.066217.

Liu, J., Ishitani, M., Halfter, U., Kim, C.S., and Zhu, J.K. (2000). The Arabidopsis thaliana SOS2 gene encodes a protein kinase that is required for salt tolerance. Proc. Natl. Acad. Sci. USA **97**:3730–3734. https://doi.org/10.1073/pnas.060034197.

Liu, L., Cui, F., Li, Q., Yin, B., Zhang, H., Lin, B., Wu, Y., Xia, R., Tang, S., and Xie, Q. (2011). The endoplasmic reticulum-associated degradation is necessary for plant salt tolerance. Cell Res. **21**:957–969. https://doi.org/10.1038/cr.2010.181.

Liu, Z., Luo, Q.H., Wen, G.Q., Wang, J.M., Li, X.F., and Yang, Y. (2015). VDAC2 involvement in the stress response pathway in *Arabidopsis thaliana*. Genet. Mol. Res. **14**:15511–15519. https://doi.org/10.4238/2015.December.1.1.

Malamy, J.E., and Benfey, P.N. (1997). Organization and cell differentiation in lateral roots of *Arabidopsis thaliana*. Development **124**:33–44. https://doi.org/10.1242/dev.124.1.33.

Marcu, M.G., Doyle, M., Bertolotti, A., Ron, D., Hendershot, L., and Neckers, L. (2002). Heat shock protein 90 modulates the unfolded protein response by stabilizing IRE1alpha. Mol. Cell Biol. **22**:8506–8513. https://doi.org/10.1128/MCB.22.24.8506-8513.2002.

Massa, G.D., and Gilroy, S. (2003). Touch modulates gravity sensing to regulate the growth of primary roots of *Arabidopsis thaliana*. Plant J. **33**:435–445. https://doi.org/10.1046/j.1365-313x.2003.01637.x.

Miyasaka, S.C., and Hawes, M.C. (2001). Possible role of root border cells in detection and avoidance of aluminum toxicity. Plant Physiol. **125**:1978–1987. https://doi.org/10.1104/pp.125.4.1978.

Moussaieff, A., Rogachev, I., Brodsky, L., Malitsky, S., Toal, T.W., Belcher, H., Yativ, M., Brady, S.M., Benfey, P.N., and Aharoni, A. (2013). High-resolution metabolic mapping of cell types in plant roots. Proc. Natl. Acad. Sci. USA **110**:E1232–E1241. https://doi.org/10.1073/pnas.1302019110.

Munns, R., and Tester, M. (2008). Mechanisms of salinity tolerance. Annu. Rev. Plant Biol. **59**:651–681. https://doi.org/10.1146/annurev.arplant.59.032607.092911.

Nagano, A.J., Fukao, Y., Fujiwara, M., Nishimura, M., and Hara-Nishimura, I. (2008). Antagonistic jacalin-related lectins regulate the size of ER body-type beta-glucosidase complexes in Arabidopsis thaliana. Plant Cell Physiol. **49**:969–980. https://doi.org/10.1093/pcp/pcn075.

Nawy, T., Lee, J.Y., Colinas, J., Wang, J.Y., Thongrod, S.C., Malamy, J.E., Birnbaum, K., and Benfey, P.N. (2005). Transcriptional profile of the Arabidopsis root quiescent center. Plant Cell **17**:1908–1925. https://doi.org/10.1105/tpc.105.031724.

Ndimba, B.K., Chivasa, S., Simon, W.J., and Slabas, A.R. (2005). Identification of Arabidopsis salt and osmotic stress responsive proteins using two-dimensional difference gel electrophoresis and mass spectrometry. Proteomics **5**:4185–4196. https://doi.org/10.1002/pmic.200401282.

Ninmanont, P., Wongchai, C., Pfeiffer, W., and Chaidee, A. (2021). Salt stress of two rice varieties: root border cell response and multi-logistic quantification. Protoplasma **258**:1119–1131. https://doi.org/10.1007/s00709-021-01629-x.

Oliveros, J.C. (2007). Venny. An Interactive Tool for Comparing Lists with Venn's Diagrams. https://bioinfogp.cnb.csic.es/tools/venny/index.html.

Petersson, S.V., Johansson, A.I., Kowalczyk, M., Makoveychuk, A., Wang, J.Y., Moritz, T., Grebe, M., Benfey, P.N., Sandberg, G., and Ljung, K. (2009). An auxin gradient and maximum in the Arabidopsis root apex shown by high-resolution cell-specific analysis of IAA distribution and synthesis. Plant Cell **21**:1659–1668. https://doi.org/10.1105/tpc.109.066480.

Petricka, J.J., Schauer, M.A., Megraw, M., Breakfield, N.W., Thompson, J.W., Georgiev, S., Soderblom, E.J., Ohler, U., Moseley, M.A., Grossniklaus, U., et al. (2012). The protein expression landscape of the Arabidopsis root. Proc. Natl. Acad. Sci. USA **109**:6811–6818. https://doi.org/10.1073/pnas.1202546109.

Qiao, Y.-X. (2011). Effects of NaCl on generation of root border cells in cucumber (*Cucumis sativus* L.). Plant Physiol. Commun. 97–101.

Qiu, Q.S., Guo, Y., Quintero, F.J., Pardo, J.M., Schumaker, K.S., and Zhu, J.K. (2004). Regulation of vacuolar Na+/H+ exchange in *Arabidopsis thaliana* by the salt-overly-sensitive (SOS) pathway. J. Biol. Chem. **279**:207–215. https://doi.org/10.1074/jbc.M307982200.

Ramireddy, E., Hosseini, S.A., Eggert, K., Gillandt, S., Gnad, H., von Wirén, N., and Schmülling, T. (2018). Root Engineering in Barley: Increasing Cytokinin Degradation Produces a Larger Root System, Mineral Enrichment in the Shoot and Improved Drought Tolerance. Plant Physiol. **177**:1078–1095. https://doi.org/10.1104/pp.18.00199.

Rasool, S., Hameed, A., Azooz, M.M., Muneeb-u-Rehman, Siddiqi, T.O., and Ahmad, P. (2013). Salt Stress: Causes, types and responses of plants. In Ecophysiology and Responses of Plants under Salt Stress, P. Ahmad, M. Azooz, and M. Prasad, eds. (Springer). https://doi.org/10.1007/978-1-4614-4747-4_1.

Rengasamy, P. (2006). World salinization with emphasis on Australia. J. Exp. Bot. **57**:1017–1023. https://doi.org/10.1093/jxb/erj108.

Reyes-Impellizzeri, S., and Moreno, A.A. (2021). The Endoplasmic Reticulum Role in the Plant Response to Abiotic Stress. Front. Plant Sci. **12**, 755447. https://doi.org/10.3389/fpls.2021.755447.

Rich-Griffin, C., Eichmann, R., Reitz, M.U., Hermann, S., Woolley-Allen, K., Brown, P.E., Wiwatdirekkul, K., Esteban, E., Pasha, A., Kogel, K.H., et al. (2020). Regulation of cell type-specific immunity networks in Arabidopsis roots. Plant Cell **32**:2742–2762. https://doi.org/10.1105/tpc.20.00154.

Rodriguez, M.C., Mehta, D., Tan, M., and Uhrig, R.G. (2021). Quantitative proteome and PTMome analysis of *Arabidopsis thaliana* root responses to persistent osmotic and salinity stress. Plant Cell Physiol. **62**:1012–1029. https://doi.org/10.1093/pcp/pcab076.

Salas-Muñoz, S., Rodríguez-Hernández, A.A., Ortega-Amaro, M.A., Salazar-Badillo, F.B., and Jiménez-Bremont, J.F. (2016). *Arabidopsis AtDjA3* null mutant shows increased sensitivity to abscisic Acid, aalt, and osmotic stress in germination and post-germination stages. Front. Plant Sci. **7**:220. https://doi.org/10.3389/fpls.2016.00220.

Shelden, M.C., and Munns, R. (2023). Crop root system plasticity for improved yields in saline soils. Front. Plant Sci. **14**:1120583. https://doi.org/10.3389/fpls.2023.1120583.

Song, R.F., Li, T.T., and Liu, W.C. (2021). Jasmonic acid impairs Arabidopsis seedling salt stress tolerance through MYC2-mediated repression of *CAT2* expression. Front. Plant Sci. **12**, 730228. https://doi.org/10.3389/fpls.2021.730228.

Su, W., Liu, Y., Xia, Y., Hong, Z., and Li, J. (2011). Conserved endoplasmic reticulum-associated degradation system to eliminate mutated receptor-like kinases in Arabidopsis. Proc. Natl. Acad. Sci. USA **108**:870–875. https://doi.org/10.1073/pnas.1013251108.

Su, N., Wu, Q., Chen, J., Shabala, L., Mithöfer, A., Wang, H., Qu, M., Yu, M., Cui, J., and Shabala, S. (2019). GABA operates upstream of H+-ATPase and improves salinity tolerance in Arabidopsis by enabling cytosolic K+ retention and Na+ exclusion. J. Exp. Bot. **70**:6349–6361. https://doi.org/10.1093/jxb/erz367.

Swarup, R., Kramer, E.M., Perry, P., Knox, K., Leyser, H.M.O., Haseloff, J., Beemster, G.T.S., Bhalerao, R., and Bennett, M.J. (2005). Root gravitropism requires lateral root cap and epidermal cells for transport and response to a mobile auxin signal. Nat. Cell Biol. **7**:1057–1065. https://doi.org/10.1038/ncb1316.

Tracy, F.E., Gilliham, M., Dodd, A.N., Webb, A.A.R., and Tester, M. (2008). NaCl-induced changes in cytosolic free Ca2+ in *Arabidopsis thaliana* are heterogeneous and modified by external ionic composition. Plant Cell Environ. **31**:1063–1073. https://doi.org/10.1111/j.1365-3040.2008.01817.x.

van Zelm, E., Zhang, Y., and Testerink, C. (2020). Salt tolerance mechanisms of plants. Annu. Rev. Plant Biol. **71**:403–433. https://doi.org/10.1146/annurev-arplant-050718-100005.

Winter, D., Vinegar, B., Nahal, H., Ammar, R., Wilson, G.V., and Provart, N.J. (2007). An "Electronic Fluorescent Pictograph" browser for exploring and analyzing large-scale biological data sets. PLoS One **2**:e718. https://doi.org/10.1371/journal.pone.0000718.

Witzel, K., and Matros, A. (2020). Fructans are differentially distributed in root tissues of asparagus. Cells **9**:1943. https://doi.org/10.3390/cells9091943.

Witzel, K., Matros, A., Bertsch, U., Aftab, T., Rutten, T., Ramireddy, E., Melzer, M., Kunze, G., and Mock, H.P. (2021). The Jacalin-related lectin HvHorcH is involved in the physiological response of barley roots to salt stress. Int. J. Mol. Sci. **22**, 10248. https://doi.org/10.3390/ijms221910248.

Xiang, Y., Lu, Y.H., Song, M., Wang, Y., Xu, W., Wu, L., Wang, H., and Ma, Z. (2015). Overexpression of a *Triticum aestivum Calreticulin* gene (*TaCRT1*) improves salinity tolerance in tobacco. PLoS One **10**, e0140591. https://doi.org/10.1371/journal.pone.0140591.

Xu, F., Copeland, C., and Li, X. (2015). Protein immunoprecipitation using *Nicotiana benthamiana* transient expression system. Bio-protocol **5**:e1520.

Xuan, W., Band, L.R., Kumpf, R.P., Van-Damme, D., Parizot, B., De Rop, G., Opdenacker, D., Möller, B.K., Skorzinski, N., Njo, M.F., et al. (2016). Cyclic programmed cell death stimulates hormone signaling and root development in Arabidopsis. Science **351**:384–387. https://doi.org/10.1126/science.aad2776.

Yang, Y., and Guo, Y. (2018). Elucidating the molecular mechanisms mediating plant salt-stress responses. New Phytol. **217**:523–539. https://doi.org/10.1111/nph.14920.

Yang, Y., Han, X., Ma, L., Wu, Y., Liu, X., Fu, H., Liu, G., Lei, X., and Guo, Y. (2021). Dynamic changes of phosphatidylinositol and phosphatidylinositol 4-phosphate levels modulate H^+-ATPase and Na^+/H^+ antiporter activities to maintain ion homeostasis in Arabidopsis under salt stress. Mol. Plant **14**:2000–2014. https://doi.org/10.1016/j.molp.2021.07.020.

Zhang, J., Liu, D., Zhu, D., Liu, N., and Yan, Y. (2021). Endoplasmic reticulum subproteome analysis reveals underlying defense mechanisms of wheat seedling leaves under salt stress. Int. J. Mol. Sci. **22**:4840. https://doi.org/10.3390/ijms22094840.

Zhou, H., Lin, H., Chen, S., Becker, K., Yang, Y., Zhao, J., Kudla, J., Schumaker, K.S., and Guo, Y. (2014). Inhibition of the Arabidopsis salt overly sensitive pathway by 14-3-3 proteins. Plant Cell **26**:1166–1182. https://doi.org/10.1105/tpc.113.117069.